Molecular Crystals and Liquid Crystals Science and Technology. Section A. Molecular Crystals and Liquid Crystals

Publication details, including instructions for authors and subscription information:
http://www.tandfonline.com/loi/gmcl19

Light Diffusion in Oriented Nematic Liquid Crystals

Bart A. van Tiggelen [a] , Anne Heiderich [a] & Roger Maynard [a]

[a] CNRS/Laboratoire de Physique et Modélisation des Systèmes Condensés, Université Joseph Fourier, Maison des Magistères, B.P. 166, 38042, Grenoble, Cedex, 9, France

Version of record first published: 04 Oct 2006

To cite this article: Bart A. van Tiggelen, Anne Heiderich & Roger Maynard (1997): Light Diffusion in Oriented Nematic Liquid Crystals, Molecular Crystals and Liquid Crystals Science and Technology. Section A. Molecular Crystals and Liquid Crystals, 293:1, 205-238

To link to this article: http://dx.doi.org/10.1080/10587259708042773

Mol. Cryst. Liq. Cryst., 1997, Vol. 293, pp. 205–238
Reprints available directly from the publisher
Photocopying permitted by license only

Light Diffusion in Oriented Nematic Liquid Crystals

BART A. VAN TIGGELEN, ANNE HEIDERICH
and ROGER MAYNARD

CNRS/Laboratoire de Physique et Modélisation des Systèmes Condensés, Université Joseph Fourier, Maison des Magistères, B.P. 166, 38042 Grenoble Cedex 9, France

(Received 16 July 1996; In final form 20 November 1996)

We study multiple light scattering from thermal fluctuations in the ordered phase of nematic liquid crystals. This state of condensed matter is characterized by long-range fluctuations of the local director, which are known to originate from bend, splay and twist deformations. This gives rise to a complicated polarization dependence of the "single-scattering" phase function, of which the consequences in multiple scattering will be discussed. In order to understand multiple scattering by long-range fluctuations in the dielectric constant, we first solve the Dyson and Bethe-Salpeter Equation for a scalar field amplitude in a self-consistent way. The diffusion constant is obtained numerically from the Kubo Greenwood formula. We compare the outcome with an approach based on point-like fluctuations. In the second part we take the tensorial aspects into account and solve the vector Bethe-Salpeter equation for light scattering caused by the De Gennes $1/q^2$ Structure factor for the director fluctuations. Using a Kubo-Greenwood formula for vector waves, we calculate diffusion tensor and transport mean free path ℓ^* of the light. Due to uniaxial birefringence the transport mean free path is no longer given by the conventional Boltzmann formula $\ell^* = \ell_{scat}/(1 - \langle\cos\theta\rangle)$. The consequences for the angular incoherent transmission (of the universal form (ℓ^*/L) $(1/2 + 3\cos\theta/4)$ will be investigated. Finally, we discuss the time-dependence of the thermal fluctuations in the context of the recent development of Diffusing Wave Spectroscopy initiated by Wolf and Maret.

Keywords: Light scattering; liquid crystals; diffusion

PACS Number(s): 42.25.Bs, 42.25.Lc, 61.30.Gd

I. INTRODUCTION

In nematic liquid crystals it is known that fluctuations in the dielectric constant (and hence the scattering of light) are completely caused by oriental

fluctuations of the local director [1]. The dielectric correlation function is given by,

$$\Gamma_{ijkl}(\mathbf{r}) \equiv \langle \varepsilon_{ij}(\mathbf{0})\, \varepsilon_{kl}(\mathbf{r}) \rangle = \frac{\varepsilon_a^2 kT/4\pi K_1}{r} \exp(-r/\xi) \prod_{ijkl}. \tag{1}$$

The amplitude of the thermal fluctuations depends on the elastic constant K_1 and the uniaxial dielectric anisotropy ε_a. The latter is typically very small: $\varepsilon_a^2 kT/8\pi K_1 \approx 10^{-5}$ μm. In a typical magnetic field of one Tesla the correlation length ξ is finite and of the order of 5 μm. This is 5 to 50 times longer than in typical Mie scattering experiments. We see that the fluctuations are both weak but with long-range nature. The tensor Π_{ijkl} addresses the tensorial aspects and will be fully acknowledged in the second part of this paper. It gives rise to unconventional selection rules for polarization transitions, which constitutes the second reason why nematic liquid crystal are so fascinating to study with light. In the first part of this paper we will replace the tensor Π_{ijkl} by 1 and investigate the role of long range correlation.

After pioneering work by De Gennes [2], single light-scattering experiments have successfully been interpreted using such a long-range correlation function, both elastic [3] and quasi-elastic ones [4]. However, very few multiple scattering studies have been carried out sofar for oriented nematic states of disordered matter [5] [6] [7], experimentally because the mean free path is large (typically millimeters) and one needs at least a centimeter sample to enter the multiple scattering domain. This is difficult because large samples tend to fall apart into "multi-domains", which each have a different direction of the average director. Such media are very interesting, but one may expect to loose the global anisotropy in light scattering. One has recently overcome these technical difficulties and light diffusion studies in oriented nematic liquid crystals have been started [6] [8]. The theory in this paper does not apply to multi-domain phases, and concentrates on the oriented phase.

On the theoretical side one may remark that the correlation length ξ is usually much smaller than the scattering mean free path, and henceforth treat multiple scattering caused by the long-range correlation function (1) with an ordinary equation of radiative transfer. Especially in Russian literature, multiple-scattering modifications of the famous De Gennes cross-section have been obtained in this way [9]. Sofar, most analyses of multiple scattering phenomena have been successfully performed using short-range and "white-noise" models. The long-range nature of the fluctuations in liquid crystals may offer new insight in multiple scattering of light. In this

paper we shall continue the theoretical study of multiple scattering from the correlation function given in Eq. (1) by concentrating on the *extreme* limit of multiple scattering: diffusion. Some results of the vector theory have already appeared in Ref. [10] and independently by Stark and Lubensky [11], and seem to agree with the recent first experiments [8].

From the problem of quantum-mechanical electron-impurity scattering it is known, both theoretically and experimentally, that the solution of the Bethe-Salpeter for the average two-particle Green's function is, on scales much longer than the mean free path, equivalent to a diffusion equation. The (energy dependent) diffusion constant is given by the Einstein relation, which establishes the fundamental relation between diffusion and conductivity. The conductivity is expressed as a Kubo-Greenwood formula, which also emerges from linear-response treatments. For a good summary we refer to the book by Mahan [12]. For classical waves several subtle modifications are known [13] [14] which become of extreme importance if resonant scattering is present. Because scattering is weak, they are not relevant here.

The scalar theory in this paper will enable us to put constraints on the validity of perturbational vector calculations, for which more advanced methods need considerable more computer time. As it turns out, several specific elements in the vector model can be understood qualitatively in the much simpler scalar picture, such as the impact of long range fluctuations. The vector theory in this paper can be compared to Monte-Carlo simulations [15] and hopefully to future experiments. The validity of the diffusion approximation in anisotropic media remains to be verified experimentally.

II. SCALAR TRANSPORT THEORY

In this section we ignore the polarization aspects, described by in Eq. (1). In that case light scattering in nematic liquid crystal reduces to a scalar theory of long-range fluctuations. We emphasize that this approximation is probably very bad, but a good understanding of the scalar theory enables us to judge in – and output of the far more sophisticated vector theory.

The structure factor is given by,

$$\Gamma(\mathbf{q}) = \frac{8\pi\Lambda}{q^2 + 1/\xi^2}. \tag{2}$$

We found it convenient to introduce the length $\Lambda = \varepsilon_a^2 kT/8\pi K_1$. Despite the smallness of the length Λ this structure factor can nevertheless be large at

forward scattering. In the scalar version of our theory we shall also adopt an isotropic free energy, and put the Franck elastic constants for bend, splay and twist all equal to each other.

In the rest of this section we shall assume that the dielectric constant of the host medium is unity. In typical liquid crystals, the range of the fluctuations ξ is much longer than in conventional Mie scattering. Perhaps future materials will exist that have even longer correlation lengths. For this reason we shall investigate when the fluctuations can be said to be "small" and "local" and subsequently described by the equation of radiative transfer, with all known consequences.

A. Average Amplitude

In this section we solve the Dyson equation for the average Green's function $G(\omega, \mathbf{p})$ at frequency ω and wave number $\mathbf{p}$, which reads in momentum space ($c = 1$):

$$G(\omega, \mathbf{p}) = \frac{1}{\omega^2 - \mathbf{p}^2 - \Sigma(\omega, \mathbf{p})}. \tag{3}$$

Since the length Λ in Eq. (1) is very small compared to the wavelength, we could suppose that the first Born approximation for the self energy $\Sigma(\omega, \mathbf{p})$ will be sufficient [7] [16],

$$\Sigma_B(\omega, \mathbf{p}) = \omega^4 \sum_{\mathbf{p}'} \Gamma(\mathbf{p}' - \mathbf{p})\, G_0(\omega, \mathbf{p}'). \tag{4}$$

Here $G_0(\omega, \mathbf{p}) = 1/[\omega^2 - p^2 + i0]$ is the vacuum (retarded) Green's function, $\Sigma_{\mathbf{p}}$ stands for $\int d^3\mathbf{p}/(2\pi)^3$ and $\Gamma(\mathbf{p})$ is the Fourier transform of $\Gamma(\mathbf{r})$. This expression (as well as some exact higher orders) for the self energy also shows up in the perturbational treatment of the Fröhlich polaron [17] where the long-range correlation function $\Gamma(\mathbf{q}) \propto 1/\mathbf{q}^2$ is taken over by electron-phonon coupling. The momentum integral in Eq. (4) can best be done by transforming it first to real space. The result is,

$$\Sigma_B(\omega, \mathbf{p}) = \frac{\omega^4 \Lambda}{p}\left[\arctan[(\omega - p)\xi] - \arctan[(\omega + p)\xi]\right.$$

$$\left. + \frac{i}{2}\log\frac{\xi^2(\omega - p)^2 + 1}{\xi^2(\omega + p)^2 + 1}\right]. \tag{5}$$

Real and imaginary part of this self energy have been shown dashed in Figures 1 and 2. The strong momentum dependence reminds us of the long range nature of the fluctuations. For $\xi \to \infty$ we infer that the real part has a first-order discontinuity at the shell $p = \omega$. At the same time the imaginary part diverges logarithmically. This catastrophe implies that the first Born approximation must break down near this point, at least if ξ is large enough. The singularity has a simple geometrical interpretation. At the point $p = \omega$ it originates from the overlap between frequency surface and the singular region of the correlation function. This geometrical argument also applies when the dispersion surface is no longer spherical. In lower dimensions the catastrophe would be even stronger than logarithmic.

Before we deal with an improvement, let us first investigate the excitations of the waves within the first Born approximation. Writing the self

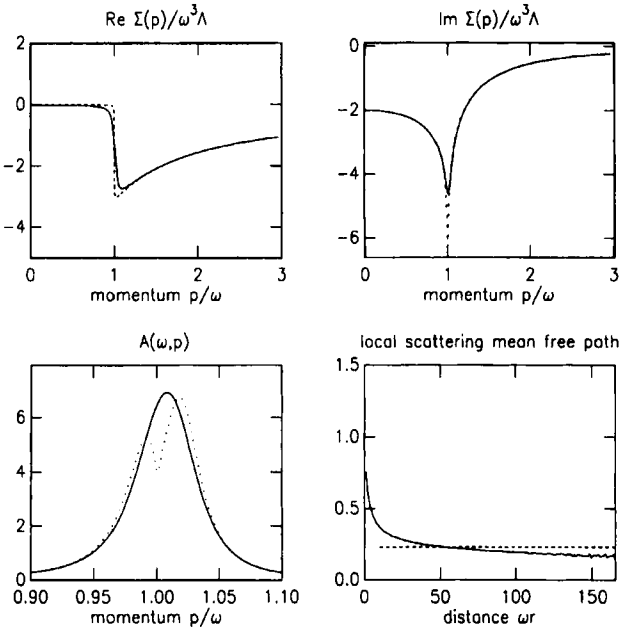

FIGURE 1 Real part of the scalar self energy (top left), imaginary part of the scalar self energy (top right), spectral function (bottom left) and the "local scattering mean free path" (bottom right), defined as $\ell(r) = -2\log(4\pi r|G(r)|)$. The dashed line in the first three plots represents the first-order Born approximation, the solid line is the self-consistent solution after 5 iterations of Eq. (10). The dashed horizontal line $\omega\ell = 23$ (i.e. $\ell \ll \xi$) in the bottom left figure is a RMS fit to a pure exponential Green's function, but note that the Green's function does not decay strictly exponentially. We chose $\omega\Lambda = 0.01$ and $\omega\xi = 1000$. The length scales Λ and ξ are introduced in the text. Note that the present values for both are considerably larger than is typically the case in nematic liquid crystals.

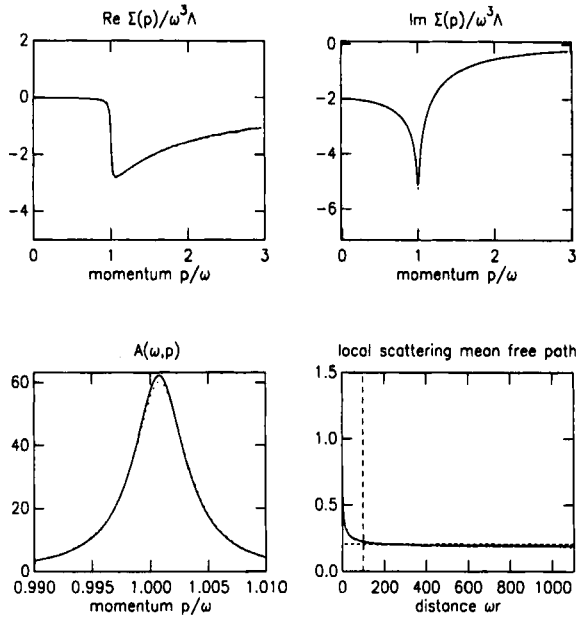

FIGURE 2 As in Figure 1 but now using $\omega\Lambda = 0.001$ and $\omega\xi = 100$ (locating the vertical dashed line). We deduce a scattering mean $\omega\ell = 200$ i.e. $\ell = 2\xi$, in good agreement with Eq. (8). Since $\omega\Lambda \ll 1/\omega\xi$, the first-order Born approximation works very well for this case. Typical liquid crystals have slightly smaller values for $\omega\Lambda$ and its validity was seen to be even better.

energy as an analytic function of p by means of the complex logarithm, the poles of the Dyson Green's function are given by,

$$\omega^2 - p^2 + \frac{i\Lambda\omega^4}{p}[\mathrm{Log}(\xi^{-1} - i\omega - ip) - \mathrm{Log}(\xi^{-1} - i\omega + ip)] = 0. \qquad (6)$$

If $\omega\Lambda \ll 1/\omega\xi$ its complex solution $K(\omega)$ is,

$$K(\omega) \approx \omega + \frac{i\omega^2\Lambda}{2}\mathrm{Log}(1 - 2i\omega\xi). \qquad (7)$$

Defining the average index of refraction m and the scattering mean free path ℓ as $K \equiv m\omega + i/2\ell$ leaves us with,

$$m(\omega) = 1 + \frac{\omega\Lambda}{2}\arctan 2\omega\xi;\ \ell(\omega) = \frac{2}{\omega^2\Lambda\,\mathrm{Log}(1 + 4\omega^2\xi^2)} \quad (\omega\Lambda \ll 1/\omega\xi). \qquad (8)$$

In a nematic liquid crystal exposed to a magnetic field **B** it is known that $\xi \propto B^{-1}$ [1]. As a result both the index of refraction and the scattering mean free path depend weakly on the magnetic field according to $m \propto T \arctan B^{-1}\ell \propto T^{-1}\omega^2/\log B$. Inserting typical values ($\omega\Lambda = 10^{-4}$ and $\omega\xi = 100$) gives us $m \approx 1 + 10^{-4}$ and $\ell \approx 0.1$ mm at optical frequencies.

The Fourier transform of the Dyson Green's function into real space can be done using contour integration in the upper sheet, thereby avoiding the branch point $\omega + i/\xi$. Obviously the complex pole (7) gives rise to a pure exponential, $G_p(\mathbf{r}) = -\exp(im\omega r - r/\ell)/4\pi r$. The integral around the branch point contributes at least a decay of $\exp(-r/\xi)$, but is not purely exponential. Its contribution can be neglected if $\ell \gg \xi$ being consistent with our previous assumption that $\omega\Lambda \ll 1/\omega\xi$. We conclude that as long as $\omega\Lambda \ll 1/\omega\xi$, or the scattering mean free path much longer than the correlation length, a first-order perturbational treatment of the complex dispersion law describes the average amplitude accurately.

The case $\omega\Lambda \gg 1/\omega\xi$ corresponds to extreme long-range correlation. To be in this regime the correlation length must have the extremely large value of $\xi \approx 1$ mm, being sofar rather unrealistic from the experimental point of view. The scattering mean free path calculated with the perturbational formula (8) is shorter than the correlation length. The problem becomes more clear by inspection of the spectral function,

$$A(\omega, \mathbf{p}) = -\frac{2\omega}{\pi} \operatorname{Im}\, G(\omega, \mathbf{p}). \tag{9}$$

In Figure 1 we demonstrate that when $\omega\Lambda \gg 1/\omega\xi$ the spectral function (in the first Born approximation, shown as a dashed line) looses weight near the conventional propagation region $\omega \approx p$. In fact the familiar Lorentzian shape of the spectral function, which can be taken as the characterization of the excitations, is suppressed exactly at its original maximum, and seems to split up into a double peak. This double peak is not predicted by the complex dispersion law (6). To verify the stability of this suppression in higher order perturbation theory, we have solved the self energy numerically in the *self-consistent* Born approximation,

$$\sum_{\mathrm{SB}}(\omega, \mathbf{p}) = \omega^4 \sum_{\mathbf{p}'} \frac{\Gamma(\mathbf{p}' - \mathbf{p})}{\omega^2 - \mathbf{p}'^2 - \Sigma_{\mathrm{SB}}(\omega, \mathbf{p}')}. \tag{10}$$

This equation has been successfully applied to model the density of states in liquid metals [18]. We emphasize that this method is approximative, and

cases exist where the first-order iteration turns out better than a self-consistent generalization. One attractive theoretical advantage of the self-consistent Born approximation is that it allows, despite its complexity, to have control over energy conservation. Such explicit conservation is necessary to address long-range diffusion, to be discussed in section II.B.

We have solved Eq. (10) iteratively, starting with the first Born approximation, until good convergence was reached. Five iterations turned out to be sufficient. Using the final solution of $\Sigma_{SB}(\omega, \mathbf{p})$ we calculated the spectral function and the Green's function in real space. In Figure 1 we show the result for $\omega\Lambda = 0.01$ and $\omega\xi = 1000$. We observe that the discontinuity in the real part of the self energy, as well as the logarithmic singularity of the imaginary part both have disappeared. Also the double peak in the spectral function is eliminated in higher order perturbation theory. We notice that the asymptotic decay of the Dyson Green's function is not purely exponential, as has been shown earlier in the limit $\omega\Lambda \ll 1/\omega\xi$. This is reflected in the "radial dependence" of the scattering mean free path, defined by means the logarithm of the Green's function. The dashed line nevertheless gives an RMS estimate of the mean free path, assuming pure exponential decay. The deduced value of $\omega\ell = 23$ is larger than expected on the basis of the simple perturbation formula (8). In Figure 2 we show a five-fold iteration of Eq. (10) for $\omega\Lambda = 0.001$ and $\omega\xi = 100$. In this case the first Born approximation has already been shown to be accurate. Indeed the iteration hardly deviates from the first Born approximation. However, some small oscillations in the real part of the self energy at $p > \omega$ seem to emerge. They were seen to be stable against further iteration. We don't know if these oscillations are just an artifact of our self-consistent approximation.

B. Diffusion Constant

Due to conservation laws, diffusive behavior may be expected in the extreme multiple-scattering domain, that is on scales much bigger than the mean free path. In this section we calculate the diffusion constant $D(\omega)$ for waves in the presence of long-range fluctuations. In isotropic media the diffusion constant can be separated into a dynamic part (the transport velocity v_E) and a stationary part (the transport meanfree path ℓ^*),

$$D(\omega) = \frac{1}{3} v_E \ell^*. \tag{11}$$

Contrary to the scattering mean free path (which is defined physically only if the Green's function decays exponentially), the transport mean free path

does not loose its meaning for extreme long-range correlation. It can been shown that $v_E \approx c/m(\omega) \approx 1$ so that the transport mean free path can be found from $D(\omega) = \ell^*/3$.

To find D we must solve the Bethe-Salpeter equation for the average two-particle Green's function [16] which reads,

$$\langle G(\omega^+, \mathbf{p}^+) G(\omega^-, \mathbf{p}^-) \rangle = G(\omega^+, \mathbf{p}^+) G(\omega^-, \mathbf{p}^-) \cdot \left[1 + \sum_{\mathbf{p}'} U_{\mathbf{pp}'}(\omega, \Omega, \mathbf{q}) \langle G(\omega^+, \mathbf{p}'^+) G(\omega^-, \mathbf{p}'^-) \rangle \right]. \tag{12}$$

Here $\mathbf{p}^\pm = \mathbf{p} \pm \mathbf{q}/2$ and $\omega^\pm = \omega \pm \Omega/2 \pm i0$; The matrix element $U_{\mathbf{pp}'}(\omega, \Omega, \mathbf{q})$ denotes the irreducible vertex. An important fact is that energy conservation gives rise to a rigorous "Ward Identity" between the self-energy and the irreducible vertex,

$$\sum(\omega, \mathbf{p}^+) - \sum^*(\omega, \mathbf{p}^-) = \sum_{\mathbf{p}'} [G(\omega, \mathbf{p}'^+) - G^*(\omega, \mathbf{p}'^-)] U_{\mathbf{pp}'}(\omega, \mathbf{q}) \tag{13}$$

If we take for the vertex in our problem "single scattering" from "one long-range fluctuation" (that is the static structure factor),

$$U_{\mathbf{pp}'}(\omega, \mathbf{q}) = \omega^4 \Gamma(\mathbf{p} - \mathbf{p}') = \frac{8\pi\omega^4 \Lambda}{(\mathbf{p} - \mathbf{p}')^2 + 1/\xi^2}, \tag{14}$$

we can infer that the self-consistent solution (10) fulfills the requirement (13) of energy conservation. This guarantees the solution of Eq. (12) to be in diffusion form,

$$\langle G(\omega^+, \mathbf{p}^+) G(\omega^-, \mathbf{p}^-) \rangle \propto \frac{1}{-i\Omega + D(\omega)\mathbf{q}^2} \quad (\Omega, \mathbf{q} \to 0). \tag{15}$$

An outstanding property of the vertex (14) is that it scatters the waves anisotropically. The diffusive solution of the Bethe-Salpeter equation (12) with *short-range* fluctuations is well-known, and yields ($|\mathbf{k}| = \omega$)

$$\frac{1}{\ell_B^*(\omega)} = \int d^2\hat{\mathbf{k}} \frac{U_{\mathbf{kk}'}(\omega)}{(4\pi)^2} (1 - \hat{\mathbf{k}} \cdot \hat{\mathbf{k}}'). \tag{16}$$

Naively inserting Eq. (14) gives,

$$\ell_B^* = \frac{1}{\omega^2 \Lambda}\left[1 - \frac{1}{2(\omega\xi)^2}\log\sqrt{1+4(\omega\xi)^2}\right]^{-1}. \tag{17}$$

This formula gives a typical value for the transport mean free path ℓ_B^* in an ordered nematic liquid crystal ranging from 0.86 mm (PAA at 125°) to 3.2 mm (MBBA at 22°). This length will later serve as a reference length in the vector theory.

We shall investigate the validity of expression (17) by solving the Bethe-Salpeter equation numerically. To this end we make use of the *exact* analogy between the present scalar wave problem and the electron-impurity problem, for which the exact solution for the diffusion constant is expressed by means of the Kubo-Greenwood formula [12],

$$D(\omega) = \frac{1}{3\pi N(\omega)} \sum_{\mathbf{p}} \left\{ p^2 |G(\omega, p)|^2 \gamma(\omega, p) - p^2 \frac{\partial}{\partial p^2} \operatorname{Re} G(\omega, p) \right\}. \tag{18}$$

In this formula $N(\omega)$ denotes the density of states. It is given by the momentum integral of the spectral function (9). The vertex function $\gamma(\omega, p)$ is determined by the integral equation,

$$\gamma(\omega, p) = 1 + \sum_{\mathbf{p}'} |G(\omega, p')|^2 \frac{\mathbf{p}\cdot\mathbf{p}'}{p^2} U_{\mathbf{p}\mathbf{p}'}(\omega)\gamma(\omega, p'). \tag{19}$$

This equation has been solved numerically, again in an iterative way, using the vertex (14) and the self-consistently determined self-energy (in practice it turned out to be convenient to use $\gamma_0 = -\operatorname{Im} \Sigma(\omega, p)/\omega^3\Lambda$ as a first iteration step, and not $\gamma_0 = 1$). In Figure 3 we show the convergence for $\gamma(\omega, p)$ for the choice $\omega\Lambda = 0.01$ and $\omega\xi = 1000$. After 10 iterations the solution was seen to be stable. In Figure 4 we have compared the calculated transport and scattering mean free paths with the mean free path ℓ_B^* given by Eq. (17). If the correlation length is large ($\omega\Lambda \gg 1/\omega\xi$) the calculated mean free paths become considerably bigger than predicted by Eqs. (8) and (16). If $\omega\Lambda > 0.01$ we are entering the strong coupling regime and the mean free paths become considerable larger than the value predicted by the perturbational formula (8).

On the other hand, Eq. (17) is a good approximation for ℓ^* when $\omega\Lambda \ll 1/\omega\xi$. This is a very convenient conclusion as present scattering experiments with nematic liquid crystals are in this regime. Translating back to physical variables we conclude from the scalar treatment that the first-order

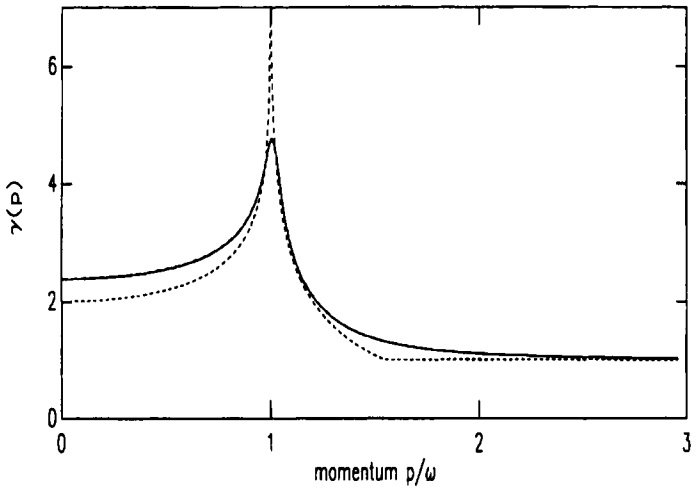

FIGURE 3 Numerical solution for $\gamma(\omega, p)$ from the scalar Bethe-Salpeter equation (19). We used the same parameters as in Figure 1. We performed 4 iterations of the Dyson equation and 10 iterations of the Bethe-Salpeter equation, of which the initial one is shown dashed and the final three in solid overlap. Using the scalar-wave Kubo-Greenwood formula (18) we obtained a transport mean free path $\ell^*/\ell_B^* = 1.053 \pm 0.002$. Numerical solution with the first-order Born self energy gives the lower value $\ell^*/\ell_B^* = 0.82$.

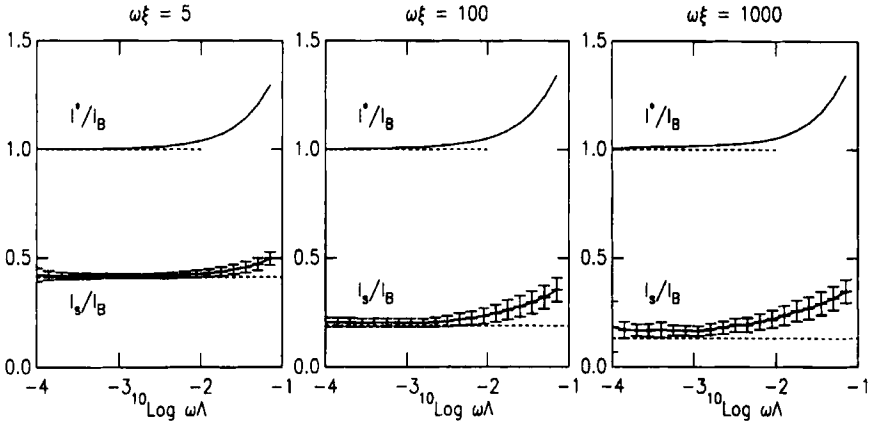

FIGURE 4 Numerical solution for transport mean free path and scattering mean free path, as a function of the relative strength of the thermal fluctuations, expressed by $\omega\Lambda$, for three different values of the correlation parameter $\omega\xi$. Dashed lines are obtained from the perturbational formulas (8) and (17). The errorbars for ℓ_S have been deduced from the standard deviation of the RMS fit to a pure exponential, including both a numerical and systematic inaccuracy. The middle figure may be said to represent a scalar picture for present nematic liquid crystals ($\omega\Lambda \approx 10^{-4}$) in the oriented phase.

perturbation theory is valid when

$$\xi < \frac{8\pi c_0^2 K_1 \sqrt{\varepsilon}}{kT\varepsilon_a^2 \omega^2}. \tag{20}$$

In a magnetic field of 1 T the right hand side equals 1 mm so that this inequality is easily obeyed. It can be checked, using approximate scaling laws for the various quantities [19] that for a very small order parameter, Eq. (20) is not violated [10]. Note that the order parameter jumps discontinuously to zero near the nematic-isotropic phase transition so that Eq. (20) holds true even very near the phase transition. In the next section we shall assume that the criterion (20) applies in a vector theory as well, so that a first-order treatment will suffice. The transport mean free path obtained in the Boltzmann approximation of the scalar theory will serve as a reference. Expressed in physical variables it reads,

$$\ell_B^* = \frac{8\pi c_0^2 K_1 \varepsilon}{kT\varepsilon_a^2 \omega^2}\left[1 - \frac{\log\sqrt{1+4\varepsilon(\omega\xi/c_0)^2}}{2\varepsilon(\omega\xi/c_0)^2}\right]^{-1}, \tag{21}$$

where ε is the dielectric constant of the host medium. As long as $\omega\xi \gg 1$ this mean free path is not very sensitive to changes in the nematic order parameter $S(\varepsilon_a \sim S$ and $K_i \sim S^2$ [19]).

III. VECTOR TRANSPORT THEORY

The exact microscopic formula for the diffusion tensor of electromagnetic waves in random media is a Kubo-Greenwood-type formula, though somewhat more difficult due to polarization indices. Although the mathematics is quite involved (see Appendix A), the basic quantity one calculates is the Fourier transform (wavenumber $\mathbf{q}$) and Laplace transform (frequency Ω) of the ensemble-averaged intensity tensor $L_{ij}(\mathbf{r},t) = \langle E_i(\mathbf{r},t)\ E_j(\mathbf{r},t)\rangle$ given a source $\delta(\mathbf{r})\ \delta(t)$. The final result is expressed as a matrix element $L_{\mathbf{pp}'}(\mathbf{q},\omega)$ describing in principle the sum of all reducibal diagrams at frequency ω, and has the singular, diffusive form for $\mathbf{q}\to 0$ and $\Omega \to 0$:

$$L_{\mathbf{pp}'}(\mathbf{q},\omega) = \frac{|\mathbf{d}(\omega,\mathbf{p},\mathbf{q})\rangle\langle\mathbf{d}(\omega,\mathbf{p}',\mathbf{q})|}{-i\Omega + \mathbf{q}\cdot\mathbf{D}(\omega)\cdot\mathbf{q}}. \tag{22}$$

For light is $L_{\mathbf{pp}'}(\mathbf{q})$ a four-rank tensor. Our tensor convention has been defined in Ref. [20]. In zero order of $\mathbf{q}$ the diffusive eigenfunction is given

by the spectral function $\mathbf{A}(\omega, \mathbf{p})$ defined as the imaginary part of the Dyson vector Green's function ($\boldsymbol{\varepsilon}$ being the dielectric tensor of the host medium),

$$\mathbf{A}(\omega, \mathbf{p}) = -\frac{2\omega}{\pi} \operatorname{Im} \mathbf{G}(\omega, \mathbf{p}) = -\frac{2\omega}{\pi} \operatorname{Im} \frac{1}{\boldsymbol{\varepsilon}\omega^2 - p^2 + \mathbf{pp} - \boldsymbol{\Sigma}(\omega, \mathbf{p})}. \tag{23}$$

The formula for the diffusion tensor $\mathbf{D}(\omega)$ is of the Kubo-Greenwood type,

$$\mathbf{q}\cdot\mathbf{D}(\omega)\cdot\mathbf{q} = \frac{1}{2\pi N(\omega)} \sum_{\mathbf{p}} \{\gamma(\mathbf{p}, \mathbf{q})\cdot\mathbf{G}(\omega, \mathbf{p})\,\mathbf{G}^*(\omega, \mathbf{p})\cdot\mathbf{L}(\mathbf{p}, \mathbf{q}) - [\mathbf{q}\cdot\partial_{\mathbf{p}}\mathbf{G}(\omega, \mathbf{p})]\cdot\mathbf{L}(\mathbf{p}, \mathbf{q})\}, \tag{24}$$

in which $\mathbf{L}(\mathbf{p}, \mathbf{q}) = 2(\mathbf{p}\cdot\mathbf{q})\ \mathbf{I} - \mathbf{pq} - \mathbf{qp}$ is a tensor of rank two, and $N(\omega)$ represents the density of states (DOS) given by ($\operatorname{Tr} \equiv \Sigma_{\text{pol}} \int d^3\mathbf{p}/(2\pi)^3$),

$$N(\omega) = \operatorname{Tr} \boldsymbol{\varepsilon}^{1/2}\cdot\mathbf{A}(\omega, \mathbf{p})\cdot\boldsymbol{\varepsilon}^{1/2}. \tag{25}$$

The ε-factors in this formula make sure that one is counting the light states as well as the states of the host-medium (in a dielectric medium the excitations concern both [14]). In terms of the irreducible vertex $U_{\mathbf{p}'\mathbf{p}}(\omega)$, the tensor $\gamma(\mathbf{p}, \mathbf{q})$, linear in $\mathbf{p}$ and $\mathbf{q}$, must obey the integral equation,

$$\gamma(\mathbf{p}, \mathbf{q}) = \mathbf{L}(\mathbf{p}, \mathbf{q}) + \sum_{\mathbf{p}'} \gamma(\mathbf{p}', \mathbf{q})\cdot\mathbf{G}(\omega, \mathbf{p}')\,\mathbf{G}^*(\omega, \mathbf{p}')\cdot U_{\mathbf{p}'\mathbf{p}}(\omega). \tag{26}$$

As soon as the Dyson self energy $\boldsymbol{\Sigma}(\omega, \mathbf{p})$ and the vertex $U_{\mathbf{p}'\mathbf{p}}(\omega)$ have been specified, this equation can be solved and the diffusion tensor can be calculated. Eq. (22) must obey the reciprocity principle

$$L_{ijkl,\,\mathbf{pp}'}(\mathbf{q}) = L_{jilk,\,-\mathbf{p}'-\mathbf{p}}(-\mathbf{q}). \tag{27}$$

On the basis of this principle one can prove that $\gamma(\mathbf{p}, \mathbf{q})$ is a symmetric tensor. For additional technical details we refer to Appendix A. In this context we note that a similar time reversal operation, as carried out in Eq. (27) leads to the tensor representation of the so-called crossed diagrams C_{ijkl} which are responsible for the coherent backscattering phenomenon [20] due to constructive interference of time-reversed pathes. The reciprocity principle gives,

$$C_{ijkl,\,\mathbf{pp}'}(\mathbf{q}) = L_{jikl,\,(\mathbf{p}-\mathbf{p}'+\mathbf{q},)/2,(\mathbf{p}'-\mathbf{p}+\mathbf{q})/2}(\mathbf{p}+\mathbf{p}'). \tag{28}$$

Thus, C can be constructed from the results in this paper. Since the phenomenon is beyond the scope of the paper it will not be discussed any further. The vector analogue of Eq. (13) for energy conservation reads

$$\sum_{\mathbf{p}'} U_{\mathbf{pp}'}(\omega)\cdot\Delta\mathbf{G}(\omega,\mathbf{p}') = \Delta\boldsymbol{\Sigma}(\omega,\mathbf{p}). \tag{29}$$

In this paper we use the notation $\Delta\mathbf{H} = \mathbf{H} - \mathbf{H}^*$.

A. Diffusion of Light in Nematic Liquid Crystals

The polarization aspects of light scattering in oriented nematic liquid crystals are characterized by a number of very special properties. First of all the oriented nematic phase has uniaxial symmetry (one optical axis $\mathbf{n}$) which gives rise to birefringence: the two modes of propagation are defined as "ordinary" and "extraordinary" with different group velocity [21]. The extraordinary mode has an ellipsoidal frequency surface $\mathbf{k}(\omega)$. If we write the dielectric tensor of the host medium as

$$\boldsymbol{\varepsilon} = \varepsilon_\perp \mathbf{I} + \varepsilon_a \mathbf{nn}, \tag{30}$$

the ordinary polarization vector and dispersion law are given by [21]

$$\mathbf{o}(\hat{\mathbf{p}}) = \hat{\mathbf{p}} \times \mathbf{n}; \quad \mathbf{k}_o(\hat{\mathbf{p}}) = \hat{\mathbf{p}}\,\omega\sqrt{\varepsilon_\perp}, \tag{31}$$

whereas the extraordinary mode has,

$$\mathbf{e}(\hat{\mathbf{p}}) = \frac{\varepsilon_\parallel(\mathbf{n}\cdot\hat{\mathbf{p}})\hat{\mathbf{p}} - (\hat{\mathbf{p}}\cdot\boldsymbol{\varepsilon}\cdot\hat{\mathbf{p}})\mathbf{n}}{\sqrt{1-(\mathbf{n}\cdot\hat{\mathbf{p}})^2}\sqrt{(\hat{\mathbf{p}}\cdot\boldsymbol{\varepsilon}^2\cdot\hat{\mathbf{p}})}}; \quad \mathbf{k}_e(\hat{\mathbf{p}}) = \hat{\mathbf{p}}\,\omega\sqrt{\frac{\varepsilon_\parallel\varepsilon_\perp}{(\hat{\mathbf{p}}\cdot\boldsymbol{\varepsilon}\cdot\hat{\mathbf{p}})}} \tag{32}$$

Secondly, the scattering of light is caused by thermal fluctuations of the local director on top of this uniaxial symmetry [1]. These fluctuations can be split up into two orthogonal modes $\delta\mathbf{n}$, both perpendicular to the optical axis. Given the wave vector $\mathbf{f} = \mathbf{k}_{in} - \mathbf{k}_{out}$ of such a fluctuation, the first mode contains bend and splay distortions and is situated in the $(\mathbf{n},\mathbf{f})$-plane; The second mode vibrates perpendicular to $\mathbf{n}$ and $\mathbf{f}$ and originates from bend and twist. The static dielectric correlation tensor contains both and is

given by [1],

$$\Gamma(\mathbf{f}) = \int d^3\mathbf{r}\, e^{i\mathbf{f}\cdot\mathbf{r}} \langle \delta\varepsilon(\mathbf{0})\, \delta\varepsilon(\mathbf{r})\rangle = \varepsilon_a^2 kT \sum_{\alpha=1,2} \frac{(\mathbf{e}_\alpha \mathbf{n})^s\, (\mathbf{e}_\alpha \mathbf{n})^s}{K_\alpha f_\perp^2 + K_3 f_\parallel^2 + \chi_a B^2}$$

$$= \frac{\varepsilon_a^2 kT/K_1}{\mathbf{f}^2 + A(\mathbf{f}\cdot\mathbf{n})^2 + 1/\xi^2} \sum_{\alpha=1,2} (\mathbf{e}_\alpha \mathbf{n})^s (\mathbf{e}_\alpha \mathbf{n})^s$$

$$\equiv 4\pi\Gamma_0(\mathbf{f}) \sum_{\alpha=1,2} (\mathbf{e}_\alpha \mathbf{n})^s (\mathbf{e}_\alpha \mathbf{n})^s. \tag{33}$$

Despite the fact that the thermal fluctuations are dynamic (section IV), the static correlation function will suffice since the characteristic time (microseconds) of the fluctuations is orders of magnitude larger than typical diffuse transit times (picoseconds). In Eq. (33) we introduced the two unit vectors $\mathbf{e}_1 = (\mathbf{f} \times \mathbf{n})/f_\perp$ and $\mathbf{e}_2 = \mathbf{n} \times \mathbf{e}_1$; K_1, K_2 and K_3 are the elastic Franck constants for splay, twist and bend deformations and are typically of the order of 10^{-11} N. In our calculations we shall rely on the "two-constant approximation" and assume that $K_1 = K_2$. The presence of a third elastic constant in the free energy will be acknowledged with $A = K_3/K_1 - 1$. This approximation conveniently decouples polarization and spatial aspects as expressed by the second equality in Eq. (33). An external magnetic field suppresses fluctuations and gives rise to a finite correlation length $\xi = \sqrt{K_1/\chi_a B^2}$. For a typical diamagnetic susceptibility $\chi_a \approx 1$ Pa/T^2 and a typical magnetic field of 1 T this length equals several microns.

The vector aspects are rather dramatic. If the host medium is sufficiently anisotropic, interference between ordinary and extraordinary waves between two collisions can be neglected. The criterion for this to hold true is $\varepsilon_a \omega \ell / \sqrt{\varepsilon_\perp} \gg 2\pi$. Since $\omega\ell \sim 10^3 - 10^4$ this inequality is satisfied. Only very near the optical axis this approximation breaks down but the contribution of this small solid angle is of higher order for the calculation of transport coefficients. The absence of interference between the two polarizations implies physically that polarization is in fact a random variable that, in a probabilistic picture, changes abruptly after each scattering.

B. Degree of Polarization

The eigenfunction $\mathbf{d}(\omega, \mathbf{p}, \mathbf{q})$ with long-range diffusion determines the degree of polarization in the multiple-scattering domain. In isotropic media one expects that $d_{ik} \sim \delta_{ik} + \mathcal{O}(p, q)$, e.g. 100% depolarized light, as shown

explicitly in Ref. [22] for Rayleigh scattering. In anisotropic media this conclusion is not valid. In general the diffuse eigenfunction is given by Eq. (23).

We shall determine the ratio of ordinary and extra-ordinary radiation after long-range diffusion. Using results in Appendix B we derive that

$$\varepsilon^{1/2}\cdot\mathbf{A}(\omega,\mathbf{p})\cdot\varepsilon^{1/2}=\mathbf{ee}\,\delta[\omega-\omega_e(\mathbf{p})]+\mathbf{oo}\,\delta[\omega-\omega_0(\mathbf{p})]. \tag{34}$$

From this relation it is easy to infer that in the diffuse domain,

$$\frac{\rho_e}{\rho_o}=\frac{d^2S_e}{|\mathbf{v}_e|}\Big/\frac{d^2S_o}{|\mathbf{v}_o|}=\left[\int d^2\hat{\mathbf{p}}\,k_e^3(\hat{\mathbf{p}})\right]\Big/\left[\int d^2\hat{\mathbf{p}}\,k_o^3\right]. \tag{35}$$

We infer that the ratio of extra-ordinary to ordinary radiation is in fact determined by the number of states available, and differs from unity. This conclusion is consistent with a semi-heuristic equipartition principle. The last identity in Eq. (35) relates the degree of polarization to the wavenumber *cubed*. Similar results have been derived by Weaver in his discussion of (S and P) elastic waves [23]. In fact the integrals in Eq. (23) are elementary and one obtains,

$$\frac{\rho_e}{\rho_o}=\frac{\varepsilon_\parallel}{\varepsilon_\perp}. \tag{36}$$

For anisotropies $\varepsilon_a \leqslant 0$ we see that ordinary radiation dominates; For positive dielectric anisotropy there will be more extra-ordinary radiation. The consequences for the diffusion constant will be discussed in the next section.

C. Diffusion Tensor

The vector self energies, both real and imaginary part as a function of momentum, in the first Born approximation have been calculated in previous work [15] [24]. Conformal our assumptions we shall write the Dyson Green's function as,

$$\mathbf{G}(\mathbf{p})=\frac{\mathbf{ee}}{\cos^2\delta_e[k_e^2(\hat{\mathbf{p}})-p^2]-\Sigma_e(\mathbf{p})}+\frac{\mathbf{oo}}{k_o^2-p^2-\Sigma_o(\mathbf{p})}+\text{rest}$$

$$\equiv g_e(\mathbf{p})\mathbf{ee}+g_o(\mathbf{p})\mathbf{oo}+\text{rest}. \tag{37}$$

The rest term contains the non-propagating longitudinal field, as well as a fluctuation-induced coupling between extraordinary and longitudinal field. Both generate high order effects in the Kubo-Greenwood formula (24) and are henceforth neglected. The angle δ_e is the angle between group and phase velocity on the extraordinary frequency surface. For the ordinary waves this angle is zero.

In the first Born approximation, the scattering vertex is [9] [16],

$$U_{\mathbf{pp}'}(\mathbf{q}) = \omega^4 \Gamma(\mathbf{p} - \mathbf{p}'). \tag{38}$$

We have to solve Eq. (26) for the tensor $\gamma(\mathbf{p}, \mathbf{q})$, and we shall write the most general bilinear form allowed by uniaxial symmetry and reciprocity,

$$\gamma(\mathbf{p}, \mathbf{q}) = 2(\mathbf{p}\cdot\mathbf{q})\,\mathbf{A}(p, c) + a(p, c)(\mathbf{pq} + \mathbf{qp}) + b(p, c)(\mathbf{n}\cdot\mathbf{p})(\mathbf{nq} + \mathbf{qn})$$
$$+ d(p, c)(\mathbf{oq} + \mathbf{qo}) + (\mathbf{n}\cdot\mathbf{p})(\mathbf{q}\cdot\mathbf{n})\,\mathbf{B}(p, c) + (\mathbf{o}\cdot\mathbf{q})\,\mathbf{D}(p, c) \tag{39}$$

The tensors **A**, **B**, and **D** and the scalars a, b and d must all be symmetrical and even functions of $c = \cos\theta = \mathbf{n}\cdot\mathbf{p}$. The "Boltzmann" solution for isotropic dielectric media with anisotropic scattering is known to be $\mathbf{A} = \mathbf{I}/(1 - \langle \hat{\mathbf{p}}\cdot\hat{\mathbf{p}}' \rangle)$, $a = -1$ and the rest zero. The imaginary part of the self energies define the scattering mean free path in direction $\hat{\mathbf{p}}$ as

$$\ell_{e/o}(\hat{\mathbf{p}}) = \frac{k_{e/o}}{-\operatorname{Im} \Sigma_{e/o}(\mathbf{k}_{e/o})} \tag{40}$$

(in the decay of the average Green's function in real space an extra factor $\cos^2\delta_{e/o}$ enters in the nominator). In lowest-order perturbation we write

$$|g_{e/o}(\mathbf{p})|^2 = \frac{\ell_{e/o}(\hat{\mathbf{p}})}{k_{e/o}(\hat{\mathbf{p}})\cos^2\delta_{e/o}(\hat{\mathbf{p}})}\,\pi\delta[k_{e/o}(\hat{\mathbf{p}})^2 - p^2].$$

After neglecting cross-terms $g_e\overline{g_o}$ it is immediately deduced that **pq**, **nq** and **oq** tensors are not generated by the integral in Eq. (26). Hence $a = -1$ and $b = d = 0$. A trace with the tensors **ee** and **oo** then provides a closed set of coupled equations for the six scalar functions $\mathbf{e}\cdot\gamma(\hat{\mathbf{p}}, \mathbf{q})\cdot\mathbf{e} \equiv \gamma_e(\hat{\mathbf{p}}, \mathbf{q}) - 2(\mathbf{e}\cdot\hat{\mathbf{p}})(\mathbf{e}\cdot\mathbf{q})$, $\mathbf{o}\cdot\gamma(\hat{\mathbf{p}})\cdot\mathbf{o} \equiv \gamma_o(\hat{\mathbf{p}}, \mathbf{q})$:

$$\gamma_e(\hat{\mathbf{p}}, \mathbf{q}) = 2(\hat{\mathbf{p}}\cdot\mathbf{q}) + \int \frac{d^2\hat{\mathbf{p}}'}{4\pi}\,\Phi_{\mathrm{EE}}(\mathbf{k}_e, \mathbf{k}'_e)[\gamma_e(\hat{\mathbf{p}}', \mathbf{q}) - 2(\mathbf{e}'\cdot\hat{\mathbf{p}}')(\mathbf{e}'\cdot\mathbf{q})].$$

$$+ \int \frac{d^2\hat{\mathbf{p}}'}{4\pi}\,\Phi_{\mathrm{EO}}(\mathbf{k}_e, \mathbf{k}'_o)\,\gamma_o(\hat{\mathbf{p}}', \mathbf{q}) \tag{41a}$$

$$\gamma_o(\hat{\mathbf{p}},\mathbf{q}) = 2(\hat{\mathbf{p}}\cdot\mathbf{q}) + \int \frac{d^2\hat{\mathbf{p}}'}{4\pi} \Phi_{OE}(\mathbf{k}_o,\mathbf{k}'_e)[\gamma_e(\hat{\mathbf{p}}',\mathbf{q}) - 2(\mathbf{e}'\cdot\hat{\mathbf{p}}')(\mathbf{e}'\cdot\mathbf{q})]. \quad (41b)$$

We introduced the scattering functions,

$$\Phi_{EE}(\mathbf{k}_e,\mathbf{k}'_e) = \frac{k'_e\ell_e(\mathbf{k}'_e)}{4\pi k_e\cos^2\delta'_e}\mathbf{e}'\mathbf{e}'\cdot\Gamma(\mathbf{k}_e-\mathbf{k}'_e)\cdot\mathbf{e}\mathbf{e} = \frac{k'_e\ell_e(\mathbf{k}'_e)\,\Gamma_0(\mathbf{k}_e-\mathbf{k}'_e)}{k_e\cos^2\delta'_e}$$

$$\times[(\mathbf{e}'\cdot\mathbf{n})^2 + (\mathbf{e}\cdot\mathbf{n})^2 - 4(\mathbf{e}'\cdot\mathbf{n})^2(\mathbf{e}\cdot\mathbf{n})^2 + 2(\mathbf{e}\cdot\mathbf{n})(\mathbf{e}'\cdot\mathbf{n})(\mathbf{e}\cdot\mathbf{e}')], \quad (42a)$$

$$\Phi_{EO}(\mathbf{k}_e,\mathbf{k}'_o) = \frac{k'_o\ell_o(\mathbf{k}'_o)}{4\pi k_e}\mathbf{o}'\mathbf{o}'\cdot\Gamma(\mathbf{k}_e-\mathbf{k}'_o)\cdot\mathbf{e}\mathbf{e} = \frac{k'_o\ell_o(\mathbf{k}'_o)}{k_e}\Gamma_0(\mathbf{k}_e-\mathbf{k}'_o)(\mathbf{e}\cdot\mathbf{n})^2, \quad (42b)$$

$$\Phi_{OE}(\mathbf{k}_o,\mathbf{k}'_e) = \frac{k'_e\ell_e(\mathbf{k}'_e)}{4\pi k_o\cos^2\delta'_e}\mathbf{e}'\mathbf{e}'\cdot\Gamma(\mathbf{k}_o,\mathbf{k}'_e)\cdot\mathbf{o}\mathbf{o}$$

$$= \frac{k'_e\ell_e(\mathbf{k}'_e)\,\Gamma_0(\mathbf{k}_o-\mathbf{k}'_e)}{k_o\cos^2\delta'_e}(\mathbf{e}'\cdot\mathbf{n})^2. \quad (42c)$$

We find that $\Phi_{OO}(\mathbf{k}_o,\mathbf{k}'_o)=0$. This feature implies an important selection rule for ordinary-ordinary polarization transitions in nematics. It is easily verified from Eqs. (41) and (42) that $\gamma_e=\gamma_o$ for $\hat{\mathbf{p}}$ parallel to the optical axis, as it should be since both polarizations degenerate in this direction.

One has three independent choices for $\mathbf{q}:\hat{\mathbf{p}}$, $\mathbf{n}$ and $\mathbf{o}$. This will enable us to determine the scalar functions $A_{e/o}$, $B_{e/o}$ and $D_{e/o}$ separately. Insertion of $\mathbf{q}=\mathbf{o}$ shows that $D_e=D_o=0$. This means that

$$\gamma_{e/o}(\hat{\mathbf{p}}\cdot\mathbf{q}) = 2(\hat{\mathbf{p}}\cdot\mathbf{q})A_{e/o}(\mathbf{n}\cdot\hat{\mathbf{p}}) + (\mathbf{q}\cdot\mathbf{n})(\mathbf{n}\cdot\hat{\mathbf{p}})B_{e/o}(\mathbf{n}\cdot\hat{\mathbf{p}}). \quad (43)$$

Closed equations for the remaining coefficients are left to Appendix B.

The final outcome can be inserted into the Kubo Greenwood formula for the diffusion tensor, again neglecting interference terms between extraordinary and ordinary modes (The second term on the right hand side of Eq. (24) is higher order *provided* we evaluate the first term near the propagative singularities only). The physics of the resulting formula is most

clearly illustrated by expressing it as an integral over the frequency surface of both modes (see also Appendix B). We find,

$$\mathbf{q}\cdot\mathbf{D}(\mathbf{n})\cdot\mathbf{q} = \frac{1}{(2\pi)^3 N(\omega)} \int \frac{d^2S_e}{|\mathbf{v}_e|} (\mathbf{v}_e\cdot\mathbf{q}) \ell_e(\hat{\mathbf{p}}) \left[\frac{1}{2}\gamma_e(\mathbf{k}_e, \mathbf{q}) - (\mathbf{e}\cdot\mathbf{q})(\mathbf{e}\cdot\hat{\mathbf{p}}) \right]$$

$$+ \frac{1}{(2\pi)^3 N(\omega)} \int \frac{d^2S_o}{|\mathbf{v}_o|} (\mathbf{v}_o\cdot\mathbf{q}) \ell_o(\hat{\mathbf{p}}) \frac{1}{2}\gamma_o(\mathbf{k}_o, \mathbf{q}) \tag{44}$$

The density of states (corrections from fluctuations can certainly be neglected here) is given by,

$$N(\omega) = \frac{1}{(2\pi)^3} \int \frac{d^2S_e}{|\mathbf{v}_e|} + \frac{1}{(2\pi)^3} \int \frac{d^2S_o}{|\mathbf{v}_o|} = \frac{1}{2\pi^2\omega} \int \frac{d^2\hat{\mathbf{p}}}{4\pi} (k_e^3(\hat{\mathbf{p}}) + k_o^3). \tag{45}$$

In the uniaxial system under consideration the diffusion tensor can be written as,

$$\mathbf{D}(\mathbf{n}) = D_\perp + (D_\parallel - D_\perp)\mathbf{nn}. \tag{46}$$

The diffusion constant along and perpendicular the optical axis can be obtained from Eq. (44) by separately choosing $\mathbf{q} = \mathbf{n}$ and integrating over all angles of $\mathbf{q}$.

In Figure 5 we show the results of our calculations. We displayed $D_\perp/D_{\text{scal}}$, $D_\parallel/D_{\text{scal}}$ and $D_\perp/D_\parallel$ as a function of the uniaxial anisotropy $\varepsilon_a/\varepsilon_\perp$; $D_{\text{scal}} = \frac{1}{3}\varepsilon_\perp^{-1/2}\ell_B^*$ is the diffusion constant obtained in the scalar theory, where ℓ_B^* was introduced in Eq. (21), and $\varepsilon_\perp^{-1/2}$ is the phase velocity in the scalar theory. In the separate plot 7 we show (the convergence of) the functions $A_{e/o}$ and $B_{e/o}$. When $\varepsilon_a/\varepsilon_\perp \gg 1$ we demonstrated in Eq. (36) that most states are extraordinary and since its frequency surface becomes very flattened along the optical axis, this case can be said to correspond to a *quasi one-dimensional* case. Therefore we expect $D_\perp$ to be small relative to $D_\parallel$. For negative anisotropies the ordinary waves dominate and we see that diffusion perpendicular to the optical axis dominates somewhat, before it becomes almost isotropic. This is consistent with the fact that the scattering mean free path for ordinary waves is anisotropic and largest perpendicular to the optical axis. The dashed line in the figure on the right shows the application of the Kubo Greenwood formula (44) in the *hypothetical* case that the angular correlations in the Bethe-Salpeter equation are neglected: $A_e = 1$ and $B_e = 0$. Apart from polarization aspects, also the anisotropy in the free energy (e.g. the sign of A) influences the anisotropy of the diffusion tensor: $A > 0$ lowers scattering along the optical axis, and thus enhances the relative importance of $D_\parallel$,

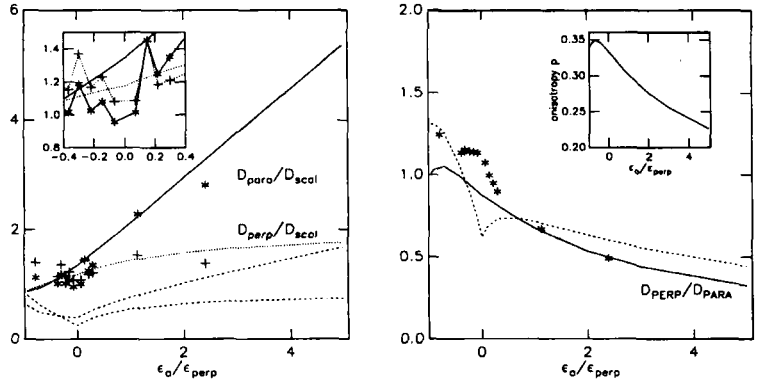

FIGURE 5 Numerical solution of the vector Bethe-Salpeter equations (41) and (44). Left: Diffusion constant parallel and perpendicular as a function of the dielectric anisotropy, $\varepsilon_a/\varepsilon_\perp$, expressed in scalar units. We took a correlation length corresponding to $\omega\xi = 63.7$ and set $A = 0.254$. The dashed line shows what would be obtained by ignoring angular correlations in the Bethe-Salpeter equation: $\gamma_{ij} = 2\mathbf{p}\cdot\mathbf{q}\delta_{ij}$. The inset shows a comparison with the calculation by an independent Monte Carlo simulation [15]. Right: the ratio $D_\perp/D_\parallel$ as a function of the same anisotropy. The dashed line again shows what is obtained by setting $\gamma_{ij} = 2\mathbf{p}\cdot\mathbf{q}\delta_{ij}$. The case $\varepsilon_a = 0$ is fictious because for this point the interference between ordinary and extraordinary waves has erroneously been neglected. The inset shows the kinematic anisotropy p of the group velocity tensor $\langle v_i v_j\rangle = p\delta_{ij} + (1-3p)n_i n_j$. ($p = 1/3$ for a single spherical frequency surface). The points show again the outcome of an independent Monte Carlo simulation [15].

described by $B_{e/o}$. This is particularly evident for PAA (Tab. I) which has long-range diffusion predominantly parallel to the optical axis.

The data points in Figure 5 have been obtained by an independent Monte-Carlo simulation [15]. The overall tendency agrees with theory, although especially for negative dielectric anisotropy quantitative discrepancies occur. This may be due to the rather big numerical uncertainty that can be deduced from the enlargement near $\varepsilon_a = 0$ (inset).

D. Diffusion Approximation for Stationary Transmission

In this subsection we calculate the transmitted light within the diffusion approximation. This approximation is supposed to be valid when the slab is

TABLE I Input data used by us for two common nematic liquid crystals, and the numerical results obtained for the diffusion tensor of the light. The relatively large value of $A = K_3/K_1 - 1$ enhances the diffusion along the optical axis. For MBBA it is less pronounced due to the smaller value for A and the compensating effect of a negative dielectric anisotropy

	$\varepsilon_\perp$	ε_a	$K_{1,2}$	A	ξ	T	$D_\perp/D_{scal}$	$D_\parallel/D_{scal}$	$D_\perp/D_\parallel$	ℓ_B^*
PAA	2.47	+0.88	3.0 pN	2.170	2.2 μm	400 K	1.613	2.824	0.571	0.28 mm
MBBA	5.40	−0.70	3.7 pN	1.014	1.5 μm	300 K	1.292	1.698	0.761	1.57 mm

sufficiently thick so that any light will have lost memory of its initial direction, i.e. the thickness L must be much larger than one transport mean free path (to be defined). In Ref. [9] one has solved the equation of radiative transfer and investigated the modifications of higher orders in scattering of the single-scattering "De-Gennes" peak in the forward direction. For low orders of scattering the diffusion approximation is not valid.

The diffusion equation for multiple scattering is well-known [25] and very successful in isotropic media. In uniaxial media it is more involved since one has to discriminate between two different modes of propagation, with different optical properties. The Stokes correlator of the electric field $\langle \mathbf{EE}^* \rangle \equiv \Phi(\mathbf{r}, \mathbf{p})$ must equal the diffusive eigenfunction derived in Eq. (A5) of Appendix A. First orders in $\mathbf{q}$ must be included because they signify the present of a net current. In real space the variable $\mathbf{q}$ transform to $-i\nabla$ so that

$$\Phi(\mathbf{r}, \mathbf{p}) = \frac{A_e(\omega, \mathbf{p})}{N(\omega)} \left\{ 1 - \frac{1}{2} \ell_e(\hat{\mathbf{p}}) [\gamma_e(\hat{\mathbf{p}}, \nabla) - 2(\mathbf{e} \cdot \nabla)(\mathbf{e} \cdot \hat{\mathbf{p}})] \right\} \Phi(\mathbf{r}) \mathbf{ee}$$

$$+ \frac{A_o(\omega, \mathbf{p})}{N(\omega)} \left\{ 1 - \frac{1}{2} \ell_o(\hat{\mathbf{p}}) \gamma_o(\hat{\mathbf{p}}, \nabla) \right\} \Phi(\mathbf{r}) \mathbf{oo}, \tag{47}$$

The scalar function $\Phi(\mathbf{r})$ must obey the diffusion equation. Since energy density and current are defined by,

$$\rho(\mathbf{r}) = \sum_{\mathbf{p}} \varepsilon_{ik} \Phi_{ki}(\mathbf{r}, \mathbf{p}), \tag{48}$$

$$J_n(\mathbf{r}) = \frac{1}{2\omega^2} \sum_{\mathbf{p}} (2p_n \delta_{ik} - p_k \delta_{ni} - p_i \delta_{nk}) \Phi_{ki}(\mathbf{r}, \mathbf{p}), \tag{49}$$

it can readily be shown that $\rho(\mathbf{r}) = \Phi(\mathbf{r})$ and $\mathbf{J}(\mathbf{r}) = -\mathbf{D} \cdot \nabla \rho(\mathbf{r})$, using the Kubo Greenwood formula and some identities given in Appendix B.

Let us introduce the unit vector $\hat{\mathbf{z}}$ perpendicular to the slab, in the direction of the current. Obviously the solution for $\Phi(\mathbf{r})$ of the slab geometry must be of the form $P + Qz$ where P and Q are to be determined by boundary conditions. Following conventional techniques we shall impose them by requiring that no net flux is incident from the right of the slab, and that unit flux is incident from the left. Fluxes $J^{\pm}$ to left and right can be defined as in Eq. (49) but with the $\hat{\mathbf{p}}$-integral restricted to the subsurfaces $S^{\pm}$ where the associated group velocity has its component along $\hat{\mathbf{z}}$ either to left

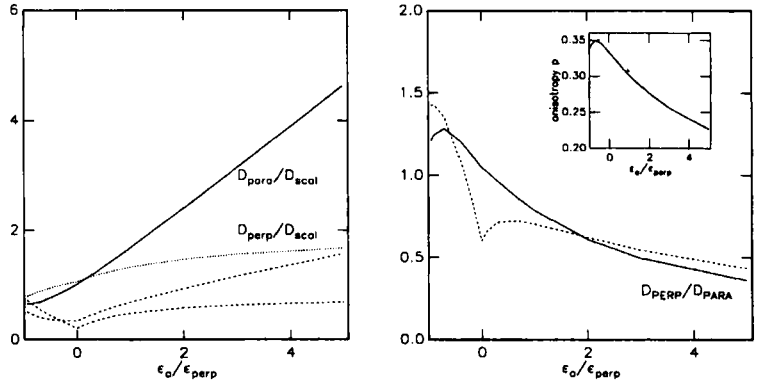

FIGURE 6 As in Figure 5 but now with a different free energy: $A = -0.254$, corresponding to a different free energy. The smaller value for A tends to suppress diffusion parallel to the optical axis.

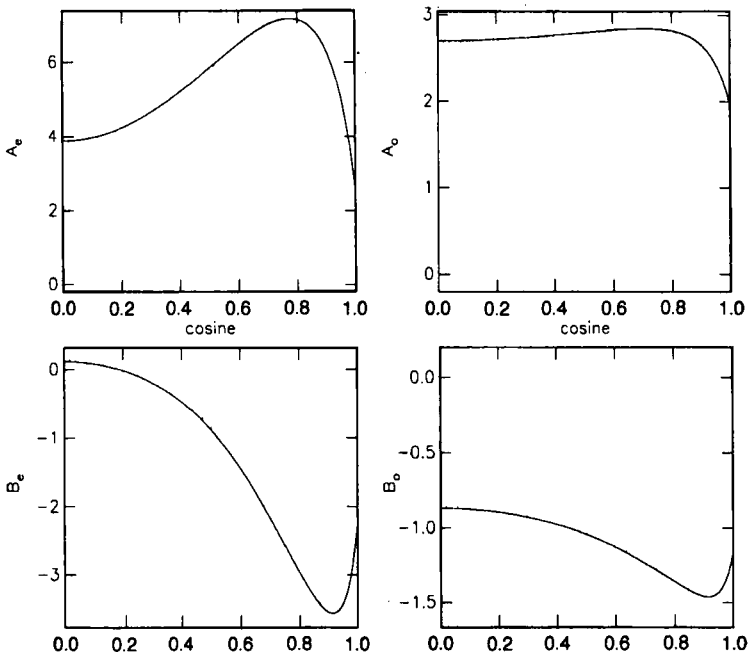

FIGURE 7 Visualization of the iterative solution of the vector Bethe-Salpeter in a nematic liquid crystal. Shown are the last 3 iterations of the angular functions $A_o(c)$, $A_e(c)$, $B_o(c)$ and $B_e(c)$, defined in Eq. 43, as a function of the cosine of the angle of the direction of propagation with the optical axis. We took $\varepsilon_a = -0.2$, $\varepsilon_\perp = 1.0$ and $\omega\xi = 63.7$ and $A = -0.254$. With the final curve (in solid) Eq. (44) yields for the diffusion tensor and $D_\parallel = 0.905\, D_{scal}$ and $D_\perp = 1.021\, D_{scal}$, where D_{scal} is the diffusion constant obtained in the scalar theory (which ignores polarization aspects and the anisotropy in free energy).

or right. In the same way the diffusion constants $D_{zz}^{\pm}$ can be introduced using the Kubo Greenwood formula (44), but on the basis of symmetry one has $D_{zz}^{\pm} = D_{zz}/2$. From the diffusive solution (47) it follows straightforwardly that,

$$J^{\pm}(z) = \frac{1}{4}\rho(z)\, v_E \mp \frac{1}{2} D_{zz}\, \partial_z \rho(z). \tag{50}$$

We introduced the scalar velocity v_E according to,

$$v_E(\mathbf{n}\cdot\hat{\mathbf{z}}) = 4\left[\int \frac{d^2 S_e^+}{|\mathbf{v}_e|}(\mathbf{v}_e\cdot\hat{\mathbf{z}}) + \int \frac{d^2 S_o^+}{|\mathbf{v}_o|}(\mathbf{v}_o\cdot\hat{\mathbf{z}})\right]\left[\int \frac{d^2 S_e}{|\mathbf{v}_e|} + \int \frac{d^2 S_o}{|\mathbf{v}_o|}\right]^{-1}, \tag{51}$$

and depends on the angle between the normal $\mathbf{Z}$ and the optical axis $\mathbf{n}$. Solving for $J^-(L) = 0$ and $J^+(0) = 1$ shows that $P = 4(L + 2D_{zz}/v_E)/(L + 4D_{zz}/v_E)$ and $Q = -4/(L + 4D_{zz}/v_E)$. This method can be generalized without difficulty to treat the birefringent reflection at both interfaces. This skin effect will not be discussed here since it depends heavily on the material outside the slab, but it influences the angular transmission profiles [26]. From Eq. (47) we can obtain the local specific intensity for ordinary and extraordinary radiation. For the extraordinary waves we define the specific intensity such that the *angular integral* $d\Omega_e$ *associated with the direction of the group velocity* gives the local current. If $K_e(\hat{\mathbf{p}})$ is the local Gaussian curvature of the extraordinary frequency surface, we have $d\Omega_e = K_e d^2 S_e / k_o^2$ [7]. The separate contributions of extraordinary and ordinary modes become,

$$\mathbf{I}_e(z,\mathbf{p}) = \frac{\hat{\mathbf{v}}_e(\hat{\mathbf{p}})\, k_o^2}{K_e(\hat{\mathbf{p}})\, n(\omega)} \frac{4}{L + 4D_{zz}/v_E}\left[L + \frac{2D_{zz}}{v_E} - z + \frac{1}{2}\ell_e(\hat{\mathbf{p}})\{\gamma_e(\hat{\mathbf{p}},\hat{\mathbf{z}}) - 2(\mathbf{e}\cdot\hat{\mathbf{p}})(\mathbf{e}\cdot\hat{\mathbf{z}})\}\right],$$

$$\mathbf{I}_o(z,\mathbf{p}) = \frac{\hat{\mathbf{v}}_o(\hat{\mathbf{p}})\, k_o^2}{n(\omega)} \frac{4}{L + 4D_{zz}/v_E}\left[L + \frac{2D_{zz}}{v_E} - z + \frac{1}{2}\ell_o(\hat{\mathbf{p}})\gamma_o(\hat{\mathbf{p}},\hat{\mathbf{z}})\right],$$

$$n(\omega) = \int \frac{d^2\hat{\mathbf{p}}\,[k_e^3(\hat{\mathbf{p}}) + k_o^3]}{\omega}. \tag{52}$$

For $z = L$ this formula gives the angular-resolved transmission coefficient. In Figures 8 and 9 we show the angular transmission $I_e(L, \mathbf{p})$ and $I_o(z, \mathbf{p})$ of extraordinary and ordinary waves, for two geometries of the nematic

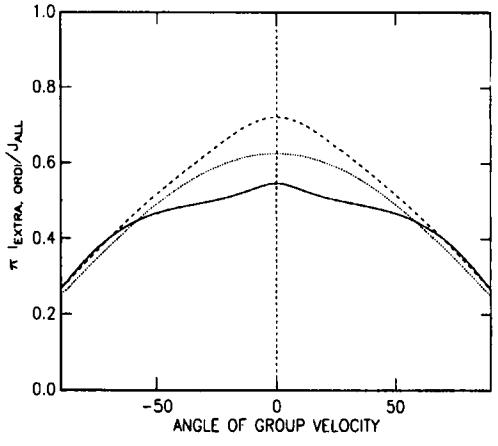

FIGURE 8 Angular transmission for MBBA obtained in the diffusion approximation. Extraordinary transmission has been shown in solid, ordinary transmission dashed, both probed in the plane of the optical axis perpendicular to the slab. The vertical dashed line signifies the location of the optical axis and is here directed perpendicular to the slab. The difference between ordinary and extra-ordinary transmission near the direction of the optical axis is due to the different solid angle with respect to which they are measured. The dotted line shows the universal formula valid $\frac{1}{4}[1 + \frac{3}{2}(\hat{\mathbf{p}} \cdot \hat{\mathbf{z}})]$ valid for isotropic media. No birefringent refraction is incorporated at the interfaces.

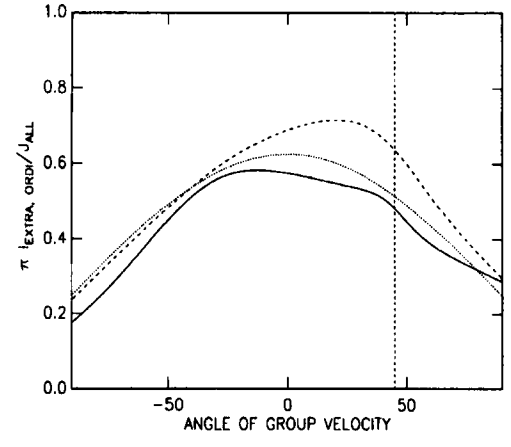

FIGURE 9 As in the previous figure but now with an inclination of 45° between slab normal and optical axis. Note the deviation from the symmetric result in isotropic media due to the presence of the optical axis.

MBBA. The angle on the horizontal axis denotes the direction of the energy flow and not the direction of $\mathbf{p}$. In the diffusion approximation, the angular dependence of $A_{e/o}(\hat{\mathbf{p}})$ and $B_{e/o}(\hat{\mathbf{p}})$ discussed earlier determines the angular shape of the diffuse transmission. This makes them *observable variables* and not only integration kernels for the diffusion tensor. Together with the angular dependence of the mean free path $\ell_{e/o}(\hat{\mathbf{p}})$ they modify the angular distribution of the diffuse transmittance, which in isotropic media is given by the *universal* formula [27] $I(L, \hat{\mathbf{p}}) \propto 1/2 + 3(\hat{\mathbf{z}}\cdot\hat{\mathbf{p}})/4$ (sometimes called the escape function). Notice that near the optical axis the specific intensities for ordinary and extra-ordinary radiation are not the same because the solid angles $d\Omega_{e,o}$ with respect to which they are measured are not the same. In addition, within an angle $d\theta \approx 1/k\ell$ with the optical axis, the interference between ordinary and extra-ordinary transmission has to be incorporated. This has not been done in the calculations.

The total transmission coefficient can be obtained by angular integration. Using the Kubo Greenwood formula (44) we find that

$$T(L) = \int d\Omega_e^+ (\mathbf{I}_e\cdot\hat{\mathbf{z}}) + \int d\Omega_o^+ (\mathbf{I}_o\cdot\hat{\mathbf{z}}) = \frac{4D_{zz}/v_E}{L + 4D_{zz}/v_E}. \tag{53}$$

This is a normal Ohmic $4\ell^*/3L$ behavior. As a matter of fact this relation enables us to *define* the *transport mean free path* as $\ell^* \equiv 3D_{zz}/v_E$. Since v_E depends on the angle between slab normal and optical axis, different geometries have different transport mean free paths, in particular

$$\frac{T_\parallel}{T_\perp} \neq \frac{D_\parallel}{D_\perp}. \tag{54}$$

This inequality is confirmed by Monte-Carlo simulations [15]. The all-angle transmission for ordinary and extraordinary modes separately can also be evaluated. Experimentally this may give information about the relative importance of both modes in the diffusion tensor. In Figure 10 we show the dependence of velocity and transport mean free path on the geometry i.e. $\hat{\mathbf{z}}\cdot\mathbf{n}$.

IV. DIFFUSING WAVE SPECTROSCOPY OF THERMAL FLUCTUATIONS

The thermally induced fluctuations of the local nematic director are dynamic. In the past, quasi-elastic light scattering experiments [4] have confirmed

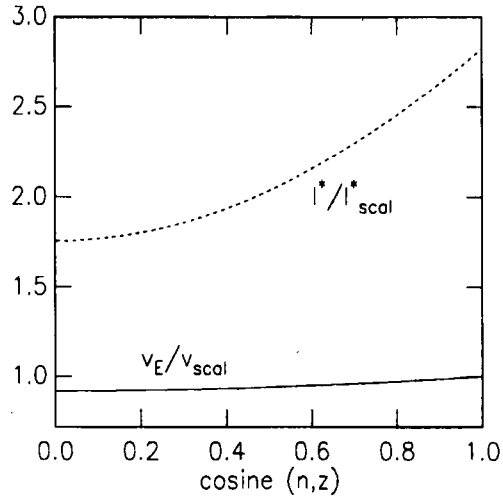

FIGURE 10 Transport velocity v_E (solid) and transport mean free path ℓ^* (dashed), figuring in the diffusion tensor $D = v_E \ell^*/3$, calculated for PAA, as a function of the cosine of the angle between optical axis and slab normal. Both have been expressed in scalar units ($v_{scal} = v_o$; ℓ^* defined in Eq. (21).

many hydrodynamic predictions for the nematic state. In this way, the Leslie kinematic viscosities in the nematic state have been determined. The typical time scales that are obtained with such experiments are of the order of milliseconds.

Quite recently, quasi-elastic experiments have been generalized to multiple scattering phenomena. The big advantage is that one can study much smaller time scales since dephasing in multiple scattering, being a collective effect, is much more sensitive to the motion of one individual scatterer. Pioneering work by Wolf and Maret [28] [29] demonstrated the utility of this new experimental technique to monitor all sorts of hydrodynamic processes. Recently one has measured such time correlations in nematic liquid crystals [8].

From the hydrodynamic continuum theory of the nematic state the following dynamic structure factor emerges [1] [30] [19],

$$\Gamma(\mathbf{q},t) = \varepsilon_a^2 kT \sum_{\alpha=1,2} \frac{(\mathbf{e}_\alpha \mathbf{n})^s (\mathbf{e}_\alpha \mathbf{n})^s}{K_\alpha q_\perp^2 + K_3 q_\parallel^2} \exp[-u_\alpha(\mathbf{q})t], \tag{55}$$

where the decay constants of both fluctuation modes are given by

$$u_1(\mathbf{q}) = \frac{K_1 q_\perp^2 + K_3 q_\parallel^2}{\lambda_1 - 2(\mu_3 q_\perp^2 - \mu_2 q_\parallel^2)^2/(\eta_s q_\perp^4 + \eta_w q_\perp^2 q_\parallel^2 + \eta_v q_\parallel^2)}, \tag{56a}$$

$$u_2(\mathbf{q}) = \frac{K_1 q_\perp^2 + K_3 q_\parallel^2}{\lambda_1 - 2\mu_2^2 q_\parallel^2/(\mu_4 q_\perp^2 + \eta_v q_\parallel^2)}. \tag{56b}$$

Characteristic is the hydrodynamic behavior of the decay constants: $u_\alpha \propto q^2$ (in the absence of magnetic field). In real space this implies a long-range $1/t^{1/2}$-decay. For a given value and direction of the scattering vector $\mathbf{q}$ the decay is exponential, but is different for the two modes. The variables $\{\mu_i\}$ denote the six Leslie viscosity coefficients in which λ_1 and $\{\eta_i\}$ can all be expressed. They have typical values of 0.005 kg/ms. Since q can be small at forward scattering, the decay is very slow there, typically milliseconds. For comparison we may consider simpler a scalar picture of the time-dependent fluctuations,

$$\Gamma(\mathbf{q}, t) = \frac{\varepsilon_a^2 kT}{K_1 q^2} \exp\left(\frac{-K_1 q^2 t}{\lambda_1}\right). \tag{57}$$

Diffusion Wave Spectroscopy consists of studying the time-dependent correlation function $\langle I(0)\, I(t)\rangle$ of the intensity in either reflection or transmission. By neglecting higher cumulants we obtain the so-called C_1-approximation for this correlation function,

$$\frac{\langle I(0)\, I(t)\rangle}{\langle I(0)\rangle^2} = 1 + \frac{|\langle \mathbf{E}(0)\cdot \mathbf{E}^*(t)\rangle|^2}{\langle I(0)\rangle^2} \equiv 1 + C_1(t) \tag{58}$$

The second term dephases when the scattering process depends on time. We shall focus on this term. The scattering vertex for the field correlation function $\langle \mathbf{E}_i(0)\, \mathbf{E}_j^*(t)\rangle$ is [31], following Eq. (38),

$$U_{\mathbf{pp}'}(\omega, t) = \omega^4 \Gamma(\mathbf{p} - \mathbf{p}', t). \tag{59}$$

On the level of the average amplitude nothing changes as a function of time since the propagation time of the light is orders of magnitude smaller than the typical fluctuation time. The self energy does therefore *not* depend on time, so that the scattering is purely elastic. This notion gives rise to the following modification of the conservation law (29),

$$\sum_{\mathbf{p}'} U_{\mathbf{pp}'}(\omega, t)\cdot \Delta \mathbf{G}(\omega, \mathbf{p}') = \Delta\Sigma(\omega, \mathbf{p}) - \mathbf{a}(\omega, \mathbf{p}, t), \tag{60}$$

where the extra term can be expressed as,

$$\mathbf{a}(\omega, \mathbf{p}, t) = \sum_{\mathbf{p}'} [U_{\mathbf{pp}'}(\omega, 0) - U_{\mathbf{pp}'}(\omega, t)] \cdot \Delta\mathbf{G}(\omega, \mathbf{p}'). \tag{61}$$

The consequences of this term for the diffusive behavior can be seen by inspection of the derivation of the Kubo Greenwood formula in Appendix A. Since we anticipate that the typical times in multiple scattering will be very small compared to the decay times of the modes it will be sufficient to consider only linear terms in t and to neglect all modifications of order a^2 and t^2. In this limit we can verify that Eq. (22) modifies to,

$$\Phi(\Omega, \mathbf{q}, t) \propto \frac{1}{-i\Omega + \mathbf{q} \cdot \mathbf{D} \cdot \mathbf{q} + a(\omega, t)}, \tag{62}$$

where

$$a(\omega, t) = \frac{1}{2\pi N(\omega)} \sum_{\mathbf{p}} \Delta\mathbf{G}^*(\omega, \mathbf{p}) \cdot \mathbf{a}(\omega, \mathbf{p}, t)$$

$$= \frac{1}{2\pi N(\omega)} \sum_{\mathbf{pp}'} \Delta\mathbf{G}^*(\omega, \mathbf{p}) \cdot [U_{\mathbf{pp}'}(\omega, 0) - U_{\mathbf{pp}'}(\omega, t)] \cdot \Delta\mathbf{G}(\omega, \mathbf{p}'). \tag{63}$$

Using Eq. (59) this expression can be evaluated numerically if all the elastic constants are known. Using the Green's function (37) the six-dimensional momentum integral can be transformed into a triple integral over incident and outgoing angle with optical axis, and azimuthal angle ϕ. We found it instructive to determine the contributions of both fluctuation modes 1 and 2 separately. We shall write,

$$a(\omega, t) = (\beta_1 + \beta_2) \times \frac{\varepsilon_a^2 kT\omega^4}{4\pi\lambda_1\sqrt{\varepsilon_\perp}} \times t + \mathcal{O}(t^2). \tag{64}$$

The second factor has the dimension of $1/s^2$. In Table II we show our computations β_1 for β_2 and for two familiar nematic liquid crystals. We conclude that their sum is of order unity, with most weight from the second mode. In the scalar simplification represented by Eq. (57) the coefficient β would be exactly unity.

If we express the diffusion tensor in terms of D_{scal} ($\mathbf{D} = \mathbf{d}D_{\text{scal}}$) as before, the normalized dephasing *in transmission* takes the form [28],

$$C_1(t) = \left(\frac{L/L_a(t)}{\sinh L/L_a(t)}\right)^2 \propto 1 - \frac{1}{3}\frac{t}{t_0} \tag{65}$$

TABLE II The dynamic viscocity λ_1 and the calculated diffusing wave coefficients β_1 and β_2 for the two modes of vibration (mode 1 in the plane of scattering vector and optical axis, mode 2 perpendicular). The other Leslie coefficients $\{\alpha_i\}$ for PAA have been taken from Table II of section 3.6 of Chandrasekhar [19]; The ones for MBBA are obtained from Table 5.1 of De Gennes [1]

	λ_1	β_1	β_2	β	$L^2(cm)\,t_0(ns)(\parallel)$	$L^2(cm)\,t_0(ns)(\perp)$
PAA	0.0068 kg/ms	0.345	0.720	1.085	5.76	3.29
MBBA	0.0763 kg/ms	0.340	0.941	1.281	393	300

(at small times), where the dephasing length is L_a and the characteristic time t_0 are given by

$$\frac{1}{L_a(t)} = \sqrt{\frac{\beta_1+\beta_2}{d_{zz}}} \times \frac{\sqrt{3}\varepsilon_a^2 kT\omega^3}{4\pi\sqrt{2\lambda_1 K_1 \varepsilon_\perp}} \times \sqrt{t} \tag{66}$$

$$t_0 = \frac{d_{zz}}{L^2} \frac{32\pi^2\lambda_1 K_1 \varepsilon_\perp}{(\beta_1+\beta_2)\varepsilon_a^4\omega^6(kT)^2}. \tag{67}$$

Inserting typical values shows that L_a is of the order of microns if t is of the order of seconds and that t_0 is of the order of nanoseconds for a slab of one centimeter. A similar $1-\gamma t/t_0$-behavior as in Eq. (65) is reported for Brownian motion of the scatterers, whereas laminar flow gives a $1-(t/t_0)^2$-behavior [32] in transmission. It would be extremely useful to probe the director fluctuations experimentally on these ultrashort time scales. It might well be possible that the hydrodynamic theory for the nematic state will break down and a different behavior will be observed.

Acknowledgements

It is a pleasure to thank Jacques Prost and Georg Maret for the stimulating discussions. This work has been supported by the Groupe de Recherche POAN.

APPENDIX A: DERIVATION OF KUBO GREENWOOD FORMULA FOR LIGHT

A microscopic transport equation for light can be obtained by considering the ensemble-averaged two-photon Green's function. Without outgoing

lines it can be expressed by the matrix element $R_{pp'}(\Omega, \mathbf{q})$. The associated Bethe-Salpeter equation for this object reads,

$$\sum_{p'} R_{pp''}(\Omega, \mathbf{q}) \cdot \{\delta_{p''p'} - Q_{p''p'}(\Omega, \mathbf{q})\} = U_{pp'}(\Omega, \mathbf{q}), \tag{A1}$$

in which,

$$Q_{p''p'}(\Omega, \mathbf{q}) \equiv \mathbf{G}\left(\omega + \frac{\Omega}{2}, \mathbf{p}'' + \frac{\mathbf{q}}{2}\right) \mathbf{G}^*\left(\omega - \frac{\Omega}{2}, \mathbf{p}'' - \frac{\mathbf{q}}{2}\right) \cdot U_{p''p'}(\Omega, \mathbf{q}).$$

From the Dyson expression for the one-photon Green's function (23) it is not difficult to see that

$$\mathbf{G}\left(\omega + \frac{\Omega}{2}, \mathbf{p}'' + \frac{\mathbf{q}}{2}\right) - \mathbf{G}^*\left(\omega - \frac{\Omega}{2}, \mathbf{p} - \frac{\mathbf{q}}{2}\right) = \mathbf{G}\left(\omega + \frac{\Omega}{2}, \mathbf{p}'' + \frac{\mathbf{q}}{2}\right)$$

$$\mathbf{G}^*\left(\omega - \frac{\Omega}{2}, \mathbf{p}'' - \frac{\mathbf{q}}{2}\right) \cdot \left\{\Sigma\left(\omega + \frac{\Omega}{2}, \mathbf{p} + \frac{\mathbf{q}}{2}\right) - \Sigma\left(\omega - \frac{\Omega}{2}, \mathbf{p} - \frac{\mathbf{q}}{2}\right)\right.$$

$$\left. + \mathbf{L}(\mathbf{p}, \mathbf{q}) - 2\omega\Omega\varepsilon\right\} \tag{A2}$$

Invoking the Ward identity (13), the integral operator $\delta_{pp''} - Q_{pp''}$ ($\Omega = 0, \mathbf{q} = \mathbf{0}$) can be seen to have an eigenvalue zero, with eigenfunction $\Delta\Sigma(\mathbf{p})$. In order to find the first perturbation in $\mathbf{q}$ and Ω it is instructive to write

$$R_{pp'}(\mathbf{q}) = \frac{K_{pp'}(\mathbf{q})}{\delta(\Omega, \mathbf{q})},$$

where we anticipate that $\delta(\Omega, \mathbf{q}) \propto -i\Omega + \mathbf{q} \cdot \mathbf{D} \cdot \mathbf{q}$. The four-rank tensor $R_{pp'}(\mathbf{q})$ must obey the reciprocity principle expressed in Eq. (27). We shall need $K_{pp'}(\mathbf{q})$ up to linear orders in $\mathbf{q}$ and write it in the symmetric form,

$$K_{pp'}(\mathbf{q}) = |\Sigma(\omega, \mathbf{p}^+) - \Sigma(\omega, \mathbf{p}^-) + \mathbf{w}(\mathbf{p}, \mathbf{q})\rangle \langle \Sigma(\omega, \mathbf{p}'^+)$$

$$- \Sigma(\omega, \mathbf{p}'^-) + \mathbf{w}(\mathbf{p}', \mathbf{q})|. \tag{A3}$$

The yet unknown second-rank tensor $\mathbf{w}(\mathbf{p}, \mathbf{q})$ must be symmetric, and linear in $\mathbf{p}$ and $\mathbf{q}$. Collecting linear orders in $\mathbf{q}$ in the Bethe-Salpeter equation (A1)

provides us with,

$$\sum_{\mathbf{p}''} \mathbf{w}(\mathbf{p},\mathbf{q})\cdot\{\delta_{\mathbf{p}''\mathbf{p}'} - Q_{\mathbf{p}\mathbf{p}''}(\mathbf{0})\} = -\sum_{\mathbf{p}''} \mathbf{L}(\mathbf{p}'',\mathbf{q})\cdot Q_{\mathbf{p}''\mathbf{p}'}(\mathbf{0}).$$

Defining $\gamma(\mathbf{p},\mathbf{q}) \equiv \mathbf{L}(\mathbf{p},\mathbf{q}) - \mathbf{w}(\mathbf{p},\mathbf{q})$ leaves us with Eq. (26). Collecting all Ω and q^2-terms gives,

$$\delta(\Omega,\mathbf{q}) = -2\pi i\Omega N(\omega) + \sum_{\mathbf{p}}\{(\gamma\,\mathbf{p},\mathbf{q})\cdot\mathbf{G}(\omega,\mathbf{p})\,\mathbf{G}^*(\omega,\mathbf{p})\cdot\mathbf{L}(\mathbf{p},\mathbf{q})$$

$$-\Delta\mathbf{G}(\omega,\mathbf{p},\mathbf{q})\cdot\mathbf{L}(\mathbf{p},\mathbf{q})\}. \tag{A4}$$

This is of the form (22) and the Kubo Greenwood formula (24) follows. The averaged two-particle Green's function is obtained by adding in and outgoing lines on both sides of $R_{\mathbf{p}\mathbf{p}'}(\mathbf{q})$. One has,

$$L_{\mathbf{p}\mathbf{p}'}(\mathbf{q}) \equiv \mathbf{G}(\omega,\mathbf{p}^+)\,\mathbf{G}^*(\omega,\mathbf{p}^-)\cdot R_{\mathbf{p}\mathbf{p}'}(\mathbf{q})\cdot\mathbf{G}(\omega,\mathbf{p}'^+)\cdot\mathbf{G}^*(\omega,\mathbf{p}'^-)$$

$$\propto \frac{|\mathbf{d}(\mathbf{p},\mathbf{q})\rangle\langle\mathbf{d}(\mathbf{p}',\mathbf{q})|}{-i\Omega + \mathbf{q}\cdot\mathbf{D}(\omega)\cdot\mathbf{q}},$$

in which the diffusive eigenfunction is, up to orders $\mathbf{q}$,

$$\mathbf{d}(\mathbf{p},\mathbf{q}) = \mathbf{A}(\omega,\mathbf{p}) - \frac{i\omega}{\pi}\gamma(\mathbf{p},\mathbf{q})\cdot\mathbf{G}(\omega,\mathbf{p})\,\mathbf{G}^*(\omega,\mathbf{p}) \tag{A5}$$

APPENDIX B: TECHNICAL DETAILS

We obtain closed equations for the six scalar functions $A_{e/o}$, $B_{e/o}$ and $D_{e/o}$ defined in Eqs. (39) and (43), suited for numerical solution. We showed already that and $a = -1$ and $b = d = 0$ and $D_{e/o} = 0$. It is instructive to express the scattered vector $\hat{\mathbf{p}}'$ in the orthonormal set $\{\mathbf{x}_1,\mathbf{x}_2,\mathbf{x}_3\} = \{\mathbf{n},(\hat{\mathbf{p}} - c\mathbf{n})/s,\mathbf{o}\}$ where $c = (\mathbf{n}\cdot\hat{\mathbf{p}})$ and $s = \sqrt{1-c^2}$, and define the azimuthal angle φ in the $\{\mathbf{x}_2,\mathbf{x}_3\}$-plane. If we take $\mathbf{q} = \mathbf{o}$ and realize that the φ-integral of Γ_0 sin φ vanishes (nothing else depends on φ) we infer indeed that

$D_e = D_o = 0$. Next, subtraction of the choice $\mathbf{q} = \hat{\mathbf{p}}$ from c times the choice $\mathbf{q} = \mathbf{n}$, and applying $\hat{\mathbf{p}} \cdot \hat{\mathbf{p}}' = cc' + ss' \cos\varphi$, leaves us with

$$A_e(c) = 1 + \int \frac{d^2\hat{\mathbf{p}}'}{4\pi} \Phi_{EE}(\mathbf{k}_e, \mathbf{k}'_e)(\mathbf{e}' \cdot \hat{\mathbf{p}}') \frac{(\mathbf{e}' \cdot \hat{\mathbf{p}}) - c(\mathbf{e}' \cdot \mathbf{n})}{s^2}$$

$$+ \int \frac{d^2\hat{\mathbf{p}}'}{4\pi} \Phi_{EE}(\mathbf{k}_e, \mathbf{k}'_e) \frac{s'}{s} \cos\varphi \, A_e(c')$$

$$+ \int \frac{d^2\hat{\mathbf{p}}'}{4\pi} \Phi_{EO}(\mathbf{k}_e, \mathbf{k}'_o) \frac{s'}{s} \cos\varphi \, A_o(c') \tag{B1a}$$

$$A_o(c) = 1 + \int \frac{d^2\hat{\mathbf{p}}'}{4\pi} \Phi_{OE}(\mathbf{k}_o, \mathbf{k}'_e)(\mathbf{e}' \cdot \hat{\mathbf{p}}') \frac{(\mathbf{e}' \cdot \hat{\mathbf{p}}) - c(\mathbf{e}' \cdot \mathbf{n})}{s^2}$$

$$+ \int \frac{d^2\hat{\mathbf{p}}'}{4\pi} \Phi_{OE}(\mathbf{k}_o, \mathbf{k}'_e) \frac{s'}{s} \cos\varphi \, A_e(c') \tag{B1b}$$

On the other hand, the difference between c times the choice $\mathbf{q} = \hat{\mathbf{p}}$ and the choice $\mathbf{q} = \mathbf{n}$ results in,

$$B_e(c) = \int \frac{d^2\hat{\mathbf{p}}'}{4\pi} \Phi_{EE}(\mathbf{k}_e, \mathbf{k}'_e) \left\{ 2\left[\frac{c'}{c} - \frac{s'}{s}\cos\varphi\right] A_e(c') - 2(\mathbf{e}' \cdot \hat{\mathbf{p}}') \frac{(\mathbf{e}' \cdot \mathbf{n}) - c(\mathbf{e}' \cdot \hat{\mathbf{p}})}{cs^2} \right\}$$

$$+ \int \frac{d^2\hat{\mathbf{p}}'}{4\pi} \Phi_{EO}(\mathbf{k}_e, \mathbf{k}'_o) 2\left[\frac{c'}{c} - \frac{s'}{s}\cos\varphi\right] A_o(c')$$

$$+ \int \frac{d^2\hat{\mathbf{p}}'}{4\pi} \Phi_{EE}(\mathbf{k}_e, \mathbf{k}'_e) \frac{c'}{c} B_e(c') + \int \frac{d^2\hat{\mathbf{p}}'}{4\pi} \Phi_{EO}(\mathbf{k}_e, \mathbf{k}'_o) \frac{c'}{c} B_o(c'), \tag{B2a}$$

$$B_o(c) = \int \frac{d^2\hat{\mathbf{p}}'}{4\pi} \Phi_{OE}(\mathbf{k}_o, \mathbf{k}'_e) \left\{ 2\left[\frac{c'}{c} - \frac{s'}{s}\cos\varphi\right] A_e(c') - 2(\mathbf{e}' \cdot \hat{\mathbf{p}}') \frac{(\mathbf{e}' \cdot \mathbf{n}) - c(\mathbf{e}' \cdot \hat{\mathbf{p}})}{cs^2} \right\}$$

$$+ \int \frac{d^2\hat{\mathbf{p}}'}{4\pi} \Phi_{OE}(\mathbf{k}_o, \mathbf{k}'_e) \frac{c'}{c} B_e(c'). \tag{B2b}$$

The integrals over φ can be carried out analytically. Conveniently we infer that the equations for $A_{e/o}(c)$ and $B_{e/o}(c)$ are in fact decoupled. Since all variables are known, Eqs. (B1) can be solved iteratively; the output serves as input for a separate iteration for Eqs. (B2).

We mention that integration over the ordinary and extraordinary frequency surface $S_{e/o}$ can be carried out according to,

$$\int d^2 S_{e/o} |\mathbf{v}_{e/o}| = \int d^2 \hat{\mathbf{p}} \frac{\omega k_{e/o}}{\cos^2 \delta_{e/o}}; \quad \int \frac{d^2 S_{e/o}}{|\mathbf{v}_{e/o}|} = \int d^2 \hat{\mathbf{p}} \frac{k_{e/o}^3}{\omega} \tag{B3}$$

where $\mathbf{v}_{e/o}$ stands for the group velocity of either mode, having the direction normal to the surface [21].

Equation (44) for the diffusion tensor, expressed as a normal angular integral, reads

$$\mathbf{q}\cdot\mathbf{D}(\mathbf{n})\cdot\mathbf{q} = \frac{1}{(2\pi)^2 N(\omega)} \int d^2 \hat{\mathbf{p}} \frac{k_e^2 \ell_e(\hat{\mathbf{p}})}{\cos^2 \delta_e} [(\hat{\mathbf{p}}\cdot\mathbf{q}) - (\mathbf{e}\cdot\mathbf{q})(\mathbf{e}\cdot\hat{\mathbf{p}})]$$

$$\cdot \left[\frac{1}{2}\gamma_e(\hat{\mathbf{p}}, \mathbf{q}) - (\mathbf{e}\cdot\mathbf{q})(\mathbf{e}\cdot\hat{\mathbf{p}})\right] + \frac{1}{(2\pi)^3 N(\omega)} \int d^2 \hat{\mathbf{p}}\, k_o^2 \ell_o(\hat{\mathbf{p}})(\hat{\mathbf{p}}\cdot\mathbf{q}) \frac{1}{2}\gamma_o(\hat{\mathbf{p}}, \mathbf{q}). \tag{B4}$$

The definitions of the scattering functions (42) and the expressions of the self-energies [15] we satisfy the normalization conventions,

$$\int d^2 \hat{\mathbf{p}} \frac{k_e^2}{\cos^2 \delta_e} \Phi_{\mathrm{EO}}(\mathbf{k}_e, \mathbf{k}'_o) = k_o^2,$$

$$\int d^2 \hat{\mathbf{p}} \frac{k_e^2}{\cos^2 \delta_e} \Phi_{\mathrm{EE}}(\mathbf{k}_e, \mathbf{k}'_e) + \int d^2 \hat{\mathbf{p}}\, k_o^2\, \Phi_{\mathrm{OE}}(\mathbf{k}_o, \mathbf{k}'_e) = \frac{(k'_e)^2}{\cos^2 \delta'_e}. \tag{B5}$$

This is in fact Eq. (29) for energy conservation, expressed in ordinary-extraordinary base.

Two useful identities in anisotropic media are Tr $\mathbf{ee}\cdot\boldsymbol{\varepsilon} = 1/|\mathbf{v}_e|^2$ and Tr $\mathbf{oo}\cdot\boldsymbol{\varepsilon} = 1/|\mathbf{v}_o|^2$ and one for the spectral function (23),

$$A_i(\omega, \mathbf{p}) = 2\omega |\mathbf{v}_i|^2\, \delta[\omega^2 - \omega_i(\mathbf{p})]^2.$$

Furthermore,

$$\frac{1}{2\omega}(2p_n\delta_{ik} - p_k\delta_{ni} - p_i\delta_{nk})\, e_i e_k = \frac{\mathbf{v}_e}{|\mathbf{v}_e|^2};$$

$$\frac{1}{2\omega}(2p_n\delta_{ik} - p_k\delta_{ni} - p_i\delta_{nk})\, o_i o_k = \frac{\mathbf{v}_o}{|\mathbf{v}_o|^2}$$

References

[1] P. G. de Gennes and J. Prost, *The Physics of Liquid Crystals*, second edition (Clarendon, Oxford, 1993).
[2] P. G. de Gennes, *Compt. Rend. Acad. Sci. Paris*, **266B**, 15 (1968).
[3] D. Langevin and M.-A. Bouchiat, *J. Phys. (Paris)*, **C1**, 197 (1975); D. Langevin, *Solid State Comm.*, **14**, 435 (1974).
[4] Orsay Liquid Crystal Group, *Phys. Rev. Lett.*, **22**, 1361 (1969).
[5] D. V. Vlasov, L. A. Zubkov, N. V. Orekhova and V. P. Romanov, *JETP Lett.*, **48**, 91 (1988). [*Pis'ma Zh. Eksp. Teor. Fiz.*, **48**, 86 (1988)].
[6] H. K. M. Vithana, L. Asfaw and D. L. Johnson, *Phys. Rev. Lett.*, **70**, 3561 (1993).
[7] V. L. Kuz'min, V. P. Romanov and L. A. Zubkov, *Phys. Rep.* **248**, 71 (1994), chapter VIII.
[8] M. H. Kao, K. A. Jester, A.G. Yodh and P. J. Collins, *Phys. Rev. Lett.*, **77**, 2233 (1996).
[9] V. P. Romanov and A. N. Shalaginov, *Opt. Spectrosc. (USSR)*, **64**, 774 (1988).
[10] B. A. van Tiggelen, R. Maynard and A. Heiderich, *Phys. Rev. Lett.*, **77**, 639 (1996).
[11] H. Stark and T. C. Lubensky, *Phys. Rev. Lett.*, **77**, 2229 (1996).
[12] G. D. Mahan, *Many Particle Physics* (Plenum, New York, 1981), section 7.1.C.
[13] M. P. van Albada, B. A. van Tiggelen, A. Lagendijk and A. Tip, *Phys. Rev. Lett.*, **66**, 3132 (1991).
[14] A. Lagendijk and B. A. van Tiggelen, *Phys. Rep.*, **270**, 143 (1996).
[15] A. Heiderich, R. Maynard and B. A. van Tiggelen, to appear in *J. Phys.* (France) II.
[16] U. Frisch, *Probabilistic Methods in Applied Mathematics*, Vol. I, edited by A. T. Bharucha-Reid, (Academic, New York, 1968).
[17] G. D. Mahan, *Many Particle Physics*, (Plenum, New York, 1981), section 6.1.
[18] L. E. Ballentine, *Adv. Chem. Phys.*, **31**, 263 (1975).
[19] S. Chandrasekhar, *Liquid Crystals*, (Cambridge, 1977).
[20] B. A. van Tiggelen, R. Maynard and Th. M. Nieuwenhuizen, *Phys. Rev. E.*, **53**, 2881 (1996).
[21] L. D. Landau, E. M. Lifshitz and L. P. Piteavskii, *Electrodynamics of Continuous Media* (Pergamon, Oxford, 1984), section XI.
[22] F. C. MacKintosh and S. John, *Phys. Rev. B.*, **37**, 1884 (1988).
[23] R. Weaver, *J. Acoust, Soc. Am.*, **71**, 1608 (1982).
[24] A. Yu. Val'kov and V. P. Romanov, *Sov. Phys. JETP*, **63**, 737 (1986).
[25] A. Ishimaru, *Wave Propagation in Random Media*, Vols. 1 and 2, (Academic, New York, 1978).
[26] M. U. Vera and D. J. Durian, *Phys. Rev. E.*, **53**, 3215 (1996).
[27] H. C. van de Hulst, *Multiple Light Scattering*, Vols. 1 and 2, (Academic, New York, 1980), see section 12.13 and Figure 11.2.
[28] P. E. Wolf and G. Maret, *Z. Phys.* B **65**, 409 (1987).
[29] D. J. Pine, D. A. Weitz, P. E. Wolf, G. Maret, E. Herholzheimer and P. M. Chaikin, in: *Scattering and Localization of Classical Waves in Random Media*, edited by Ping Sheng (World Scientific, 1990), 312.
[30] R. Schaetzing and J. D. Litster, in: *Advances in Liquid Crystals*, **4**, edited by G. H. Brown, (Academic, New York, 1979).
[31] E. Kogan, D. Eliyahu and M. Kaveh, *Z. Phys. B.*, **91**, 497 (1993).
[32] D. Bicout and R. Maynard, *Physica. B.*, **204**, 20 (1995); D. Bicout and G. Maret, *Physica. A.*, **210**, 87 (1994).